NASA TECHNICAL NOTE

NASA TN D-7758

NASA TN D-7758

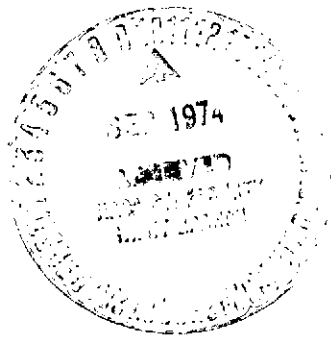

OZONE MEASUREMENT SYSTEMS IMPROVEMENTS STUDIES

by Robert W. Thomas, Keith Guard, Alfred C. Holland, and John F. Spurling

Wallops Flight Center
Wallops Island, Va. 23337

NATIONAL AERONAUTICS AND SPACE ADMINISTRATION • WASHINGTON, D. C. • AUGUST 1974

ERRATA

NASA Technical Note D-7758

OZONE MEASUREMENT SYSTEMS
IMPROVEMENT STUDIES

By Robert W. Thomas, Keith Guard, Alfred C. Holland,
and John F. Spurling

August 1974

Page 3: Line 11 replace the words "15% greater than the correct value" with "5% in error".
Line 25 replace the word "overestimated" with "underestimated".
Line 27 replace "ozone estimate so that an underestimation can occur" with "extent of the underestimation".

Page 51: Replace table 3 with attached corrected table.

Page 55: Replace page with attached corrected page.

Page 65: Replace figure 19 with attached corrected figure.

Page 67: Replace page with attached corrected figure.

Page 68: Replace figure 20 with attached corrected figure.

Page 69: Replace figure 21 with attached corrected figure.

Page 70: Replace page with attached corrected page.

Page 71: Replace figure 22 with attached corrected figure.

Page 72: Replace figure 23 with attached corrected figure.

Page 74: Lines 1 and 2 replace the first sentence with the sentence "Estimates of the total ozone by zenith sky measurements can be a few percent low, the amount of the underestimate being reduced by the presence of aerosols".

Revised Pages 51, 55, 65, 67, 68, 69, 70, 71, 72 & 74 inserted 9-16-75.

Page 77: Line 13 replace the words "15% greater than the correct value" with "5% in error, the amount".
Line 28 replace the word "overestimated" with "underestimated".
Line 30 replace word "reduce" by "increase" and "overestimated" by "underestimated".

Issued April 1975

NASA-Langley, 1975

1. Report No.	2. Government Accession No.	3. Recipient's Catalog No.
NASA TN D-7758		

4. Title and Subtitle	5. Report Date
OZONE MEASUREMENT SYSTEMS IMPROVEMENTS STUDIES	August 1974
	6. Performing Organization Code

7. Author(s)	8. Performing Organization Report No.
Robert W. Thomas and Keith Guard (Wolf Research and Development Corporation) Alfred C. Holland and John F. Spurling (NASA Wallops Flight Center)	

9. Performing Organization Name and Address	10. Work Unit No.
Wolf Research and Development Corp., 6801 Kenilworth Avenue, Riverdale, Maryland 20840 and NASA Wallops Flight Center, Wallops Island, Virginia 23337	11. Contract or Grant No. NAS6-2173

12. Sponsoring Agency Name and Address	13. Type of Report and Period Covered
National Aeronautics and Space Administration Washington, D.C. 20546	TECHNICAL NOTE
	14. Sponsoring Agency Code

15. Supplementary Notes

16. Abstract

This report summarizes the results of an initial study of techniques for measuring atmospheric ozone, carried out as the first phase of a program to improve ozone measurement techniques. The study concentrated on two measurement systems, the Electro Chemical Cell (ECC) Ozonesonde and the Dobson Ozone Spectrophotometer, and consisted of two tasks. The first task consisted of error modeling and system error analysis of the two measurement systems. Under the second task a Monte-Carlo model of the Dobson ozone measurement technique was developed and programmed for computer operation. Some results are discussed.

17. Key Words (Suggested by Author(s))

Ozone
Upper Atmosphere
Ozonometry
Measuring Instruments
Instrument Errors
Optical Equipment
Scattering
Monte Carlo Method

18. Distribution Statement

Unclassified - Unlimited

Cat. 13

19. Security Classif. (of this report)	20. Security Classif. (of this page)	21. No. of Pages	22. Price*
Unclassified	Unclassified	95	$4.00

*For sale by the National Technical Information Service, Springfield, Virginia 22151

CONTENTS

OZONE MEASUREMENT SYSTEMS IMPROVEMENTS STUDIES

by

Robert W. Thomas and Keith Guard
Wolf Research and Development Corporation

and

Alfred C. Holland and John F. Spurling
NASA Wallops Flight Center

SUMMARY

This report summarizes the results of an initial study of techniques for measuring atmospheric ozone that was carried out at NASA Wallops Station. This study represents the first phase of a program designed to improve techniques for the measurement of atmospheric ozone. The initial phase was concerned with two distinct tasks.

1) A study of the effects of atmospheric transmission parameters on ozone measurements.

2) An analysis of ozone measurement systems.

Under task 2 an analysis was performed to determine estimates of the errors in total ozone data due to errors in the Dobson measurement process, in instrument calibration and adjustment, and in the assumptions made in deriving the data reduction equations. The analysis does not include the effects of:

1) Systematic errors in determining the "extra-terrestrial constant." The use of the technique of extrapolation to zero optical path length is subject to error if the assumption of no diurnal variation in total ozone is not valid.

2) The wavelength dependence of the scattering caused by particulate matter.

3) Errors in the ozone absorption coefficients used in the data reduction.

The error in the total ozone inferred from Dobson direct sun measurements using the A, D lines, due to the factors analyzed, was estimated to be

$$\Delta X_{AD} = .010 \text{ atm-cm},$$

which is about 3% of the typical total ozone reading.

In the Electrochemical Concentration Cell (ECC) Ozonesonde an error analysis of the effects of chart measurement error and of errors in the instrument calibration and data reduction process results in an estimated error in ozone partial pressure of

$$\Delta P_3 = 4.6 \text{ } \mu\text{mb},$$

which is 2% to 3% of the peak ozone partial pressure reading.

The above analysis, however, does not include the effects of possible errors in the cell reaction equation. These errors are of undetermined magnitude, but calibration tests against standard ozone generators indicate agreement within 5%.

In the use of the ECC ozonesonde data to determine total ozone, errors of over 5% are possible, if a secondary ozone maximum exists above the peak altitude reached by the balloon borne sonde.

A limited intercomparison of data from the ECC ozonesonde and Dobson Ozone Spectrophotometer was carried out, using data collected during the Meteorological Rocket/Nimbus Satellite Data Comparison Experiment (RNSC), in the summer of 1970. The results were that total ozone data obtained from the two sources had a mean difference of 0.0005 atm.-cm., with an estimated standard deviation of 0.008 atm.-cm. However, the sample used

was quite small, using only 11 ECC measurements, and an extended program of data comparison, that would also include data from satellite-borne instruments, is recommended.

Under task 1 a Monte Carlo model of the Dobson ozone estimation was assembled and tested. The model and the associated tests employed are discussed in section 4.0. The model was used to study the effects of molecular and aerosol scattering on ozone inferred from Dobson direct sun and zenith sky observations. Our results show that in the model we have employed the total ozone estimated using the standard equations for the direct sun mode of the Dobson Spectrophotometer can be up to 15% greater than the correct value depending on the receiver field of view. The discrepancy is due to two causes:

1) A discrepancy between our model of the ozone absorption cross-section and that employed by Dobson. The results demonstrate the sensitivity of the total ozone estimate to the assumed variation of total ozone cross section with temperature, and the assumed vertical ozone and temperature profiles.

2) Single and multiple scattered radiation entering the receiver, principally radiation scattered by aerosols.

The results for the zenith sky measurements show that in our model the total ozone is overestimated by a few percent when aerosols are not present but that the effect of single and multiple scattering by aerosols is to reduce the ozone estimate so that an underestimation can occur.

In all of the results considered we found that when aerosols were present the effect of multiple scattering was as great if not greater than that of single scattering. Thus a detailed investigation of the influence of multiple scattering on the Umkehr experiment is necessary.

Recommendations - It is recommended that future work should emphasize the following items:

1) Use of Monte Carlo model to study the sensitivity of Dobson measurements to variations in ozone density and profile.

2) Study Improvements in ozone measurement techniques.

3) Use the Monte Carlo model to study satellite-based, ultra-violet back scattering techniques and their sensitivity to ozone variations.

4) Conduct an intercomparison of satellite-borne and ground-based measurement systems similar to that performed during the Rocket/Nimbus Sounder Comparison (RNSC).

INTRODUCTION

The subject of the quantity of ozone in the upper atmosphere has recently gained increased attention because of questions relating to the effect of Supersonic Transport exhaust gases on ozone concentration.

A variety of photochemical processes take place in the upper atmosphere of which only those involving the various forms of oxygen are important in determining the amount of ozone. The inference of the "equilibrium amount" of ozone is of considerable importance since the amount of ozone that is present serves to block hazardous ultra-violet radiation from reaching the earth's surface. A significant depletion in the protective layer of ozone might present hazards to human life.

However, independent of questions of atmospheric pollution, the problems of measurement and analysis to investigate the processes of ozone generation by photochemical reactions, diffusion by atmospheric processes and depletion by interaction with atmospheric trace elements have long been of interest to the scientific and meteorological communities. A primary reason for the interest is that knowledge of the processes of ozone formation and diffusion is essential to understanding of atmospheric energy exchange. As the ozone layer blocks the incoming ultra-violet radiation, it absorbs heat energy which subsequently is important as a driving mechanism of atmospheric motion.

Also, below the photochemical region, at about 30km, ozone is a conservative element in the atmosphere in the absence of pollutants, and acts as an excellent tracer for large and medium-scale atmospheric movements.

Vertical and horizontal transport mechanisms in the stratosphere and upper troposphere can be deduced by examination of vertical ozone concentration profiles.

To summarize, ozone is a particularly important trace constituent which:

1) strongly absorbs the damaging ultra-violet radiation

2) is a source of thermal energy in the stratosphere and is responsible for the increase of temperature with height

3) plays a significant role in the overall transfer of solar energy, and

4) assumes meteorological importance as a tracer to indicate atmospheric circulation.

Ozone in the Stratosphere

Ozone is formed in the upper stratosphere (below about 45 kilometers) by the photochemical action of solar ultra-violet radiations of wavelengths 1760 A.U. to 1925 A.U., by a process of disassociation of oxygen (O_2) into free oxygen atoms, and by photochemical combination of oxygen atoms and oxygen molecules into ozone. In this process the solar radiation in this band is completely absorbed. Radiation in the band of 2200 A.U. to 2900 A.U. destroys ozone, in the process of being absorbed. During daylight hours, a state of equilibrium between creation and destruction of ozone is established above about 25 kilometers, resulting in the existence of ozone at a nearly constant mixing ratio in that region.

Below 25 kilometers photochemical effects of radiation are nearly non-existent, due to the absorption of most of the radiation above that altitude. The air containing ozone is diffused downward in the stratosphere, and generally toward the poles in latitude, by atmospheric circulation processes which are still under investigation.

Within the stratosphere below 25 kilometers, ozone is considered to be a conservative element, that is, one which is neither produced nor destroyed. Ozone is very unstable and is destroyed by the chemical action of traces of water vapor or atmospheric pollutants. The concentration of these substances is negligible in the stratosphere, thus ozone is conserved.

When the stratospheric ozone is moved into the troposphere by diffusion or circulation, the ozone is rapidly diffused toward the ground and is destroyed.

Ozone Measurement Programs at Wallops Island

A program of regular weekly launchings of ozonesondes on balloons, in conjunction with radiosondes, has been in operation at Wallops Island since 1967. Initially Wallops supported a program including five AFCRL stations conducting regular ozone soundings, which was discontinued in 1969. NASA Wallops, recognizing the need for "ground truth" measurements to support experiments on board the Nimbus satellites investigated the use of an ECC ozonesonde developed by the Atmospheric Physics and Chemistry Laboratory, Boulder, Colorado. Wallops is now the only location in the United States where a regularly scheduled program of ozonesonde launch is operating.

The ECC ozonesonde provides the best currently available method for obtaining vertical ozone profiles providing structural detail to 30 or 35 km. These data are necessary if ozone structure is to be used as an atmospheric tracer, and to provide profiles to be used as approximate solutions in reduction of data from satellite-borne spectrometers or from "Umkehr" measurements with the ground-based Dobson Spectrophotometer.

Since mid-1967, a program of regular observations of total ozone, using a Dobson Spectrophotometer, has been in operation at NASA Wallops Island. The instrument was obtained on indefinite loan from NOAA since it was surplus to their needs. The observing program consists of three measurements of total ozone per day, at about 10 AM, noon, and 2 PM, local time, on a non-interfering basis to primary station activities. Weather permitting, direct sun measurements are made, otherwise zenith sky measurements are used. The Dobson instrument is a double-beam monochromator, measuring relative intensities in the solar spectrum of two neighboring

wavelengths in the ozone absorption band around 3000 Angstroms, from which can be calculated total ozone in the column of air through which the sunlight has passed. The instrument has been a measurement standard for atmospheric ozone since the early 1930's when it was first developed.

In addition to total ozone measurements made by observing direct light from the sun, the Dobson instrument can be used to obtain a first order approximation to the vertical ozone profile by the Umkehr technique. The Umkehr method uses a set of observations on the scattered sunlight from the zenith sky, taken at times when the sun is at various zenith angles ranging from 50° to 90°. Since the estimates are based on theoretical profiles for computation of absorption rates and of atmospheric scattering, the results do not reveal detailed structure.

Theoretical Studies Conducted at Wallops Station

In order to provide a basis for estimating the quality of the ozone data produced from the two measurement systems a program of theoretical studies was initiated at Wallops Station. This report summarizes the results of the first phase of that investigation. Two approaches were taken, in parallel:

1) an analytical evaluation and an error analysis of the Dobson Spectrophotometer and ozonesonde calibration, operation, and data reduction.

2) a Monte-Carlo investigation of the effects of scattering by molecules and aerosols on the results of the Dobson instrument.

The analytical investigation was intended to:

1) Provide brief reviews of operating principles and procedures, for both types of instruments.

2) Provide an evaluation of the methods of determining total ozone by the Dobson Spectrophotometer and the determination of vertical ozone concentration profiles by balloon borne ozonesondes.

3) Present the results of data intercomparisons between the systems studied to substantiate the error analysis, where possible.

The purpose of the Monte Carlo investigation was to determine the effect on the reduced ozone data from the Dobson instrument of radiative transfer phenomena, including:

1) single and multiple molecular scattering

2) single and multiple aerosol scattering.

ANALYTICAL INVESTIGATIONS

Dobson Spectrophotometer

System Description. - The Dobson Spectrophotometer is a specialized double beam monochrometer, used for determining atmospheric ozone by measuring the ratio of the intensities of two selected wavelengths of ultra violet light in the solar spectrum. The wavelength pair is selected so that one wavelength is much more strongly absorbed by ozone than the other, so that the intensity ratio can be used to estimate the total amount of ozone in the optical path from the sun to the instrument. By appropriate adjustments of the spectrophotometer one of several specified wavelength pairs can be selected for the measurement, depending on illumination conditions, to provide an estimate of the amount of atmospheric ozone.

The Dobson instrument can be used in three distinct modes; a direct sun measurement, a "zenith sky" measurement and a "Umkehr" mode. In the direct sun mode a prism or "Sun Director" is used to project the sun's image onto the entrance window of the Dobson Spectrophotometer. The direct sun mode is the preferred method for measuring total ozone. In the zenith sky mode the instrument observes radiation scattered from the zenith sky for a number of solar zenith angles less than 60 degrees. The zenith sky measurements are used when the sun is obscured by clouds. In the Umkehr mode the zenith sky measurements are made for solar zenith angles ranging from 90° to 50°.

The Dobson instrument measures the relative intensities of the two wavelengths in a given pair by first separating them in a spectroscope, isolating them with slits, and attentuating the beam at the wavelength least absorbed by ozone with a variable thickness optical filter (the filter wedge). The two beams are brought back into coincidence with a second spectroscope so that they impinge on a photo-electric null-meter. The null-meter does not measure absolute intensities, instead it indicates when the difference between the intensities is zero. The null-meter consists of a chopper wheel in the optical path, which passes the two beams sequentially and a photo-multiplier upon which one beam and then the other fall sequentially as allowed by the chopper wheel. An amplifier is used for the A.C. output of the photo-multiplier, then a rectifier which converts the alternating current to direct current, and finally a direct current micro-ammeter for display.

The ratio of the intensities of the two beams is "measured" by adjusting the filter wedge until the micro-ammeter reads zero. Then the intensity ratio is computed from the position of the filter wedge and the instrument calibration data.

Wavelength Doublet and Wavelength-Doublet Pairs. - By wavelength adjustment dial settings on the instrument, (the Q dial) one of five wavelength doublets can be chosen. Table 1 taken from Reference 1, gives data on wavelength doublets A, B, C, D and C'. At present wavelength doublet B is not used, so that only four wavelength doublets are used. Also, as is explained in the section on data reduction, when making observations for total ozone it is desirable to make nearly simultaneous observation on two wavelength doublets. The wavelength doublet pairs used are AD, CD, and CC'.

For very large zenith angles (greater than about 72°), a focused image of the sun is formed on the entrance slit of the instrument. This increases the apparent intensity of the light and decreases the effects of scattered light. For zenith angles less than 72°, a ground glass plate is placed on the instrument aperture, to diffuse the light and average the intensity over the entrance slit. For zenith angles less than 30°, the lens is removed from the sun director to further decrease the intensity of the received light.

TABLE 1 - TABLE WAVELENGTHS AND OTHER CONSTANTS
(absorption coefficients are based on $\log_{10}$)

Designation of Wavelength doublet		Mean Wavelength A.U.	Ozone Absorption Coefficient $(atm\ cm)^{-1}$ α / α'	$\alpha-\alpha'$	Atmospheric Scattering Coefficient $(atm)^{-1}$ β / β'	$\beta-\beta'$	$\frac{\beta-\beta'}{\alpha-\alpha'}$
A	Short	3055	1.882	1.762	0.491	0.116	0.066
	Long	3254	0.120		0.375		
B	Short	3088	1.287	1.223	0.470	0.113	0.092
	Long	3291	0.064		0.357		
C	Short	3114.5	0.912	0.865	0.453	0.110	0.127
	Long	3324	0.047		0.343		
D	Short	3176	0.391	0.374	0.416	0.104	0.278
	Long	3398	0.017		0.312		
C'	Short	3324	0.047	0.047	0.343		
	Long	4536	Nil				

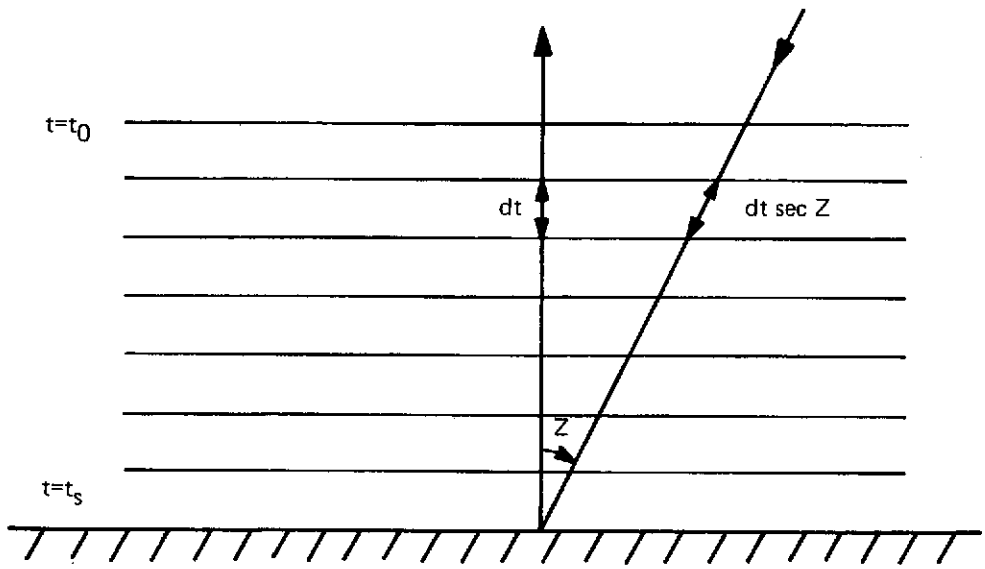

Figure 1 - Geometry of plane parallel case.

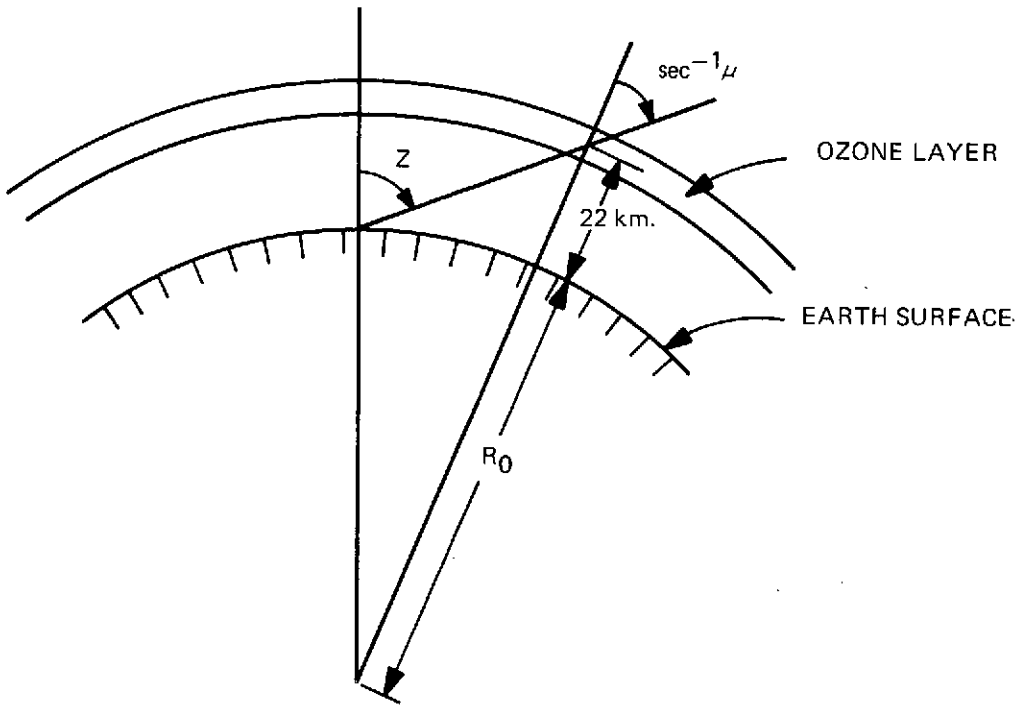

Figure 2 - Geometry for calculation of μ.

The actual measurements are recorded on a waxed disc, fitted to the R-dial, which moves the optical filter wedge back and forth. A clock-work mechanism driving an arm which carries a stylus is mounted with the pivot of the stylus just outside the radius of the R-dial. If the R-dial is left motionless, the stylus traces an arc across the waxed disc, taking about 15 minutes. In operation, the R-dial is set so that the micro-ammeter reading is nearly zero, the stylus placed in position, and the R-dial is "jittered" so that the ammeter needle swings in a small arc symmetric about the zero reading. The line traced by the stylus also oscillates about the zero reading.

Theory of Measurement Using Direct Sunlight. - For a plane-parallel stratified atmosphere (figure 1) containing Rayleigh scatterers (molecules), ozone molecules and aerosols, the change in sunlight from one layer to the next can be expressed as:

$$dI(t) = -I(t)\{\sigma_m(t)p_m(t) + \sigma_o(t)p_o(t) + \sigma_p(t)p_p(t)\}\sec Z\, dt. \quad (1)$$

The quantity I(t) denotes the intensity at altitude t while $\sigma(t)$ denotes a cross section for scattering or absorption and p(t) denotes the number of molecules or particles per cubic centimeter. Subscripts denote molecules (m) ozone molecules (0) and particles (p). Note that we have neglected any light that might be scattered into the path from other parts of the atmosphere; we only consider losses from the beam due to scattering and absorption.

Integrating the equation from the top of the sensible atmosphere (t=0) to the surface ($t=t_s$) we have:

$$\ln\left[\frac{I(t_s)}{I(0)}\right] = -\int_0^{t_s}\{\sigma_m(t)p_m(t) + \sigma_o(t)p_o(t)+\sigma_p(t)p_p(t)\}\sec Z dt. \quad (2)$$

If we now define the quantities

$$\int_0^{t_s} \sigma_m(t) p_m(t) \text{Sec } Z \, dt = \beta_m T_m \sec Z, \tag{3}$$

$$\int_0^{t_s} \sigma_p(t) p_p(t) \text{Sec } Z \, dt = \delta_p T_p \sec Z, \tag{4}$$

and

$$\int_0^{t_s} \sigma_o(t) p_o(t) \text{Sec } Z \, dt = \alpha_o X \sec Z, \tag{5}$$

then the equation for the intensity reaching the ground based instrument is:

$$\ln I(t_s) = \ln I_o - \{\beta_m T_m - \delta_p T_p - \alpha_o X\} \sec Z. \tag{6}$$

Essentially the quantity T_m represents the "scale height" of the atmosphere, that is the thickness of the molecular atmosphere if it were reduced to a uniform layer at Standard Temperature and Pressure. Similarly β_m then represents the Rayleigh volume scattering coefficient for the atmosphere at Standard Temperature and Pressure. The volume coefficient can be calculated from the Rayleigh-Cabannes formulae for the scattering cross section per molecule and Loschmidts number. The product $\beta_m T_m$ is the normal or vertical optical thickness of the atmosphere due to Rayleigh or molecular scattering. Similarly $\delta_p T_p$ represents the normal optical thickness of the atmospheric aerosol and $\alpha_o X$ represents the normal optical thickness of the ozone layer. The parameter X is the equivalent thickness of ozone or the ozone scale height, and is the quantity of interest. In this plane parallel model, restricted to zenith angles Z less than 60°, we do not concern ourselves with the effect of refraction on the path length, and we neglect the effect of the earth's curvature.

In the equations for the Dobson direct sun measurement they use an equivalent path through the atmosphere that is defined as equal to one or one air mass when the suns zenith is zero. This is tantamount to redefining the molecular scattering coefficient to be equal to the vertical optical thickness of the molecular atmosphere (one air mass). The same statement can be made regarding the particulate scattering coefficient.

Then we have:

$$\ln I(t_s) = \ln I_o - \{\beta+\delta+\alpha_o X\}\sec Z, \qquad (7)$$

where now $\beta=\beta_m T_m$ and $\delta=\delta_p T_p$.

In Dobson's derivation for the direct sun measurement the quantity sec Z multiplying the expression for the ozone optical thickness and molecular optical thickness is replaced by quantities μ and m . The parameter m is defined to be the equivalent path length through the molecular atmosphere allowing for atmospheric refraction and the curvature of the earth. When the zenith angle is zero m is defined to be 1.0.

The quantity μ is the relative path length of sunlight through the ozone layer which is presumed to be at 22 km above the earths surface. When the zenith angle is zero μ is also defined to be 1.0.

The quantity μ can be calculated (see Figure 2) from the solar zenith angle Z by

$$\mu = \frac{1}{\sqrt{1 - \left(\frac{R_o}{R_o+22}\right)^2 + \left(\frac{R_o}{R_o+22}\right)^2 \mathrm{Cos}^2 Z}}. \qquad (8)$$

R_o is the assumed radius of the earth, 6378 km.

In practice for direct sun measurements at solar zenith angles less than 60° these distinctions are unnecessary. However, for completeness we shall use Dobson's form from here on. The equation is then:

$$\ln I_\lambda = \ln I_{o\lambda} - \alpha\mu X - \beta m - \delta \sec Z. \tag{9}$$

The preceding discussion used $\log_e$, indicated by ln. Changing to $\log_{10}$, and writing equation (7) for two wavelengths λ and λ', then subtracting the two resulting equations yields Dobson's equation 2 (Reference 1):

$$\log_{10}(I/I') = \log_{10}(I_o/I_o') - (\alpha-\alpha')\mu X - (\beta-\beta')\, m - (\delta-\delta')\sec Z. \tag{10}$$

Letting

$$L_\lambda = \log_{10}(I/I') \tag{11}$$

$$L_{o\lambda} = \log_{10}(I_o/I_o'),$$

$$N_\lambda = L_{o\lambda} - L_\lambda , \tag{12}$$

yields

$$-N_\lambda = -(\alpha-\alpha')_\lambda \mu X - (\beta-\beta')_\lambda m - (\delta-\delta')_\lambda \sec Z, \tag{13}$$

and solving for X yields

$$X = (N_\lambda - (\beta-\beta')_\lambda m - (\delta-\delta')\sec Z)/(\alpha-\alpha)_\lambda \mu. \tag{14}$$

The subscript λ indicates the wavelength dependence of the terms, and prime indicates the longer wavelength.

The term containing $(\delta-\delta')$ cannot be evaluated explicitly because the attenuation coefficients for particulate scattering usually are not known. As a means of avoiding this difficulty, observations are made simultaneously on two wavelength pairs, say A and D, and the resulting equation (12) subtracted and solved for X. The result, using the values given in Table 1 is:

$$X_{AD} = .7205\ (N_A - N_D)/\mu - .009m/\mu$$
$$- ((\delta-\delta')_A - (\delta-\delta')_D)/((\alpha-\alpha')_A - (\alpha-\alpha')_D)\mu. \quad (15)$$

The last term in equation (15) has been set to be zero, on the assumption that particulate scattering coefficients are only slightly wavelength dependent, thus cancelling the two terms in the numerator. Also, the ratio m/μ in the second term is set equal to 1, with negligible effect. We then have

$$X_{AD} = 0.7205(N_A - N_D/\mu - 0.009 \quad (16)$$

Reduction of AD and CD Measurements Using Direct Sunlight. -

a) After taking the measurements as described above, obtain the R-dial readings by estimating the center of the stylus trace with respect to the 1° arcs.

b) Look up the value of N, for λ=A,C, or D corresponding to the R-dial reading from tables furnished with the instrument.

c) Use the N_λ values in the equations:

$$X_{AD} = 0.7205\ (N_A - N_D)/100\mu - 0.009, \quad (17)$$

$$X_{CD} = 2.037\ (N_C - N_D)/100\mu - 0.12. \quad (18)$$

Note: the N_λ values read from the tables are actually $100\ N_\lambda$, so the results must be divided by 100.

d) Given solar zenith angle Z, the quantity μ is computed using equation (8).

e) The solar zenith angle Z is computed from the equation

$$\cos Z = \sin d \sin \phi + \cos d \cos \phi \cos H,$$

ϕ = latitude of observing stations, (19)
d = declination of the sun,
H = hour angle of the sun.

Reduction of Measurement of Light from the Zenith Sky. - The reduction of total ozone data from zenith sky measurements is done by using empirical tables and charts, derived by making a large number of nearly simultaneous direct sun and zenith sky measurements, for different values of μ. The charts are constructed on the assumption that, for a given value of μ, a one-to-one relationship exists between total ozone and the N-values obtained from zenith sky measurements. This assumption can be justified only if the vertical distribution of ozone, and of the scatterers in the atmosphere, can be assumed to be constant with the exception of a scale factor. Since this assumption is not valid, the zenith sky reductions are subject to errors which cannot be estimated analytically, and extensive Monte-Carlo simulations will be required to provide error estimates.

Error Analysis of Reduction of Direct Sun Measurements on A, D Wavelengths. -

Basic Measurement Error: The error in R-dial measurement has been estimated by a number of reliable observers (References 1,2) to be of the order of 0.2° on the R-dial under good observing conditions, and not to exceed 0.5° under bad conditions.

The error in determination of the time of the observation may be taken as 30 seconds for normal operating methods.

Propagation of Error Through the Data Reduction Equations: The data reduction equation to be evaluated is equation (17) which is repeated here for convenience

$$X_{AD} = 0.7205(N_A - N_D)/100\mu - 0.009.$$

The propagation of error rule used is the usual chain rule differentiation, using only the linear term of the Taylor's Series expansion of the variable. The measured variables are R-dial readings R_A, R_D and time t.

$$\Delta X_{AD} = \frac{\partial X_{AD}}{\partial R_A} \Delta R_A + \frac{\partial X_{AD}}{\partial R_D} \Delta R_D + \frac{\partial X_{AD}}{\partial t} \Delta t. \qquad (20)$$

The partial derivatives in equation (20) can be evaluated as follows:

$$\frac{\partial X_{AD}}{\partial R_A} = \frac{\partial X_{AD}}{\partial N_A} \frac{\partial N_A}{\partial R_A} , \tag{21}$$

$$\frac{\partial X_{AD}}{\partial R_D} = \frac{\partial X_{AD}}{\partial N_D} \frac{\partial N_D}{\partial R_D} , \tag{22}$$

$$\frac{\partial X_{AD}}{\partial t} = \frac{\partial X_{AD}}{\partial \mu} \frac{\partial \mu}{\partial t} . \tag{23}$$

For zenith angles less than 60° μ can be approximated by

$$\mu = \frac{1}{\cos Z} , \tag{24}$$

where cos Z is obtained from equation (19).

Then

$$\frac{\delta \mu}{\delta t} = \frac{\delta \mu}{\delta (\cos Z)} \frac{\delta (\cos Z)}{\delta H} \frac{\delta H}{\delta t} , \tag{25}$$

where from equation (24)

$$\frac{\partial \mu}{\partial \cos Z} = \frac{-1}{\cos^2 Z} = -\mu^2 , \tag{26}$$

from equation (19)

$$\frac{\partial (\cos Z)}{\partial H} = \text{cosd cos}\phi \text{ sin H} , \tag{27}$$

and from the definition of H,

$$\frac{\partial H}{\partial t} = \frac{2\pi}{86,400} \frac{\text{radians}}{\text{second}} . \tag{28}$$

From equation (15)

$$\frac{\partial}{\partial \mu} = \frac{X}{\mu}, \tag{29}$$

$$\frac{\partial X_{AD}}{\partial N_A} = -.7205/100\mu \tag{30}$$

$$\frac{\partial X_{AD}}{\partial N_D} = -.7205/100\mu. \tag{31}$$

using the tables of N vs R used in data reduction,

$$\frac{\partial N_\lambda}{\partial R_\lambda} = .95 \tag{32}$$

is a reasonable average for λ = A, D.

The indicated calculations were carried out for extreme values of H, that is for H = 0° and H = 87°.

Using $\Delta R = 0.2°$ and Δt = 30 seconds, for H = 0°,

$$\Delta X_{AD} = 0.0013_{R_A} + 0.0013_{R_D} + 0.0000_t, \tag{33}$$

where the subscript indicates the error source. For H = 87°:

$$\Delta X_{AD} = 0.0004_{R_A} + 0.0004_{R_D} + .0017_t. \tag{34}$$

If it is assumed that the error sources are independent and randomly distributed about zero, and the errors on ΔR and Δt represent standard deviations about zero then the separate errors may be combined by taking the square root of the sum of the squares to obtain:

$$\sigma_{AD} = 0.0018, \text{ for } H = 0°,$$

$$\sigma_{AD} = 0.0018, \text{ for } H = 87°.$$

Similar computations can be carried out for the CD wavelength.

The results of the above computations were recorded to only two significant figures, since the basic estimates of measurement error are probably only valid within a factor of two. The result indicates that the error in reduced ozone due solely to measurement errors, and not considering instrument adjustment, calibration, or the derivation of the basic equations, is less than 1% of the total ozone.

Also, it should be emphasized that only the direct sun type of measurement is amenable to the above error analysis. The zenith sky measurements are reduced using empirical charts, obtained by comparing zenith sky measurements to direct sun measurements taken at the same zenith angle.

Instrument Calibration and Adjustment. - The discussion below is only a summary of the calibration and adjustment procedures and of the routine checks to maintain calibration for the Dobson instrument, based on reference 2.

Adjustment of the Optics: All optical components of the instrument, including lenses, prisms, slit widths are adjusted when the instrument is installed. Detailed instructions for periodic inspection and re-adjustment, if necessary, are included in Reference 4. All of the optical components are fixed in position with the exception of the wavelength adjustments Q_1 and Q_2 and the optical filter wedge. The primary sources of error, in a properly maintained instrument, will be in the adjustable components. For that reason, inspection and adjustment of the fixed optical components will not be discussed here.

Calibration of the Wavelength Adjustment Q_1 and Q_2: The various components of the instrument change dimensions slightly with temperature. These changes are compensated for by making changes in the setting of the optical flat Q_1, using a table of settings of Q_1 vs. temperature. The wavelengths A, C, and D were all selected to make the identification of the proper wavelength possible, even in the absence of optical laboratory

equipment such as precision monochromatic sources or spectrometers. Each of the wavelengths identifies itself because the ozone absorption spectrum has an inflection point at the wavelength. Thus, slight movements of the Q_1 adjustment lever about the nominal value of each of the wavelengths results in a photocell output plot, vs Q_1 setting, as shown in Figure 3, which is taken from Reference 1.

Errors Caused by Incorrect Setting of Q_1: Using the method previously described of obtaining error propagation, the errors in X caused by a Q_1 lever setting error ΔQ_1 are

$$\Delta X_{AD} = \left(\frac{\partial X_{AD}}{\partial N_A} \frac{\partial N_A}{\partial R_A} \frac{\partial R_A}{\partial Q_1} - \frac{\partial X_{AD}}{\partial N_D} \frac{\partial N_D}{\partial R_D} \frac{\partial R_D}{\partial Q_1} \right) \Delta Q_1. \tag{35}$$

All of the factors in the terms on the right of this equation was evaluated above except $\frac{\partial R_\lambda}{\mu Q_1}$, for λ=A, D.

The magnitude of these three terms can be graphically estimated from Figure 3, yielding

$$\frac{\partial R_A}{\partial Q_1} = -1.6 \frac{^\circ R_A}{^\circ Q_1}, \tag{36}$$

$$\frac{\partial R_C}{\partial Q_1} = -0.1 \frac{^\circ R_C}{^\circ Q_1}, \tag{37}$$

$$\frac{\partial R_D}{\partial Q_1} = -1.2 \frac{^\circ R_D}{^\circ Q_1}, \tag{38}$$

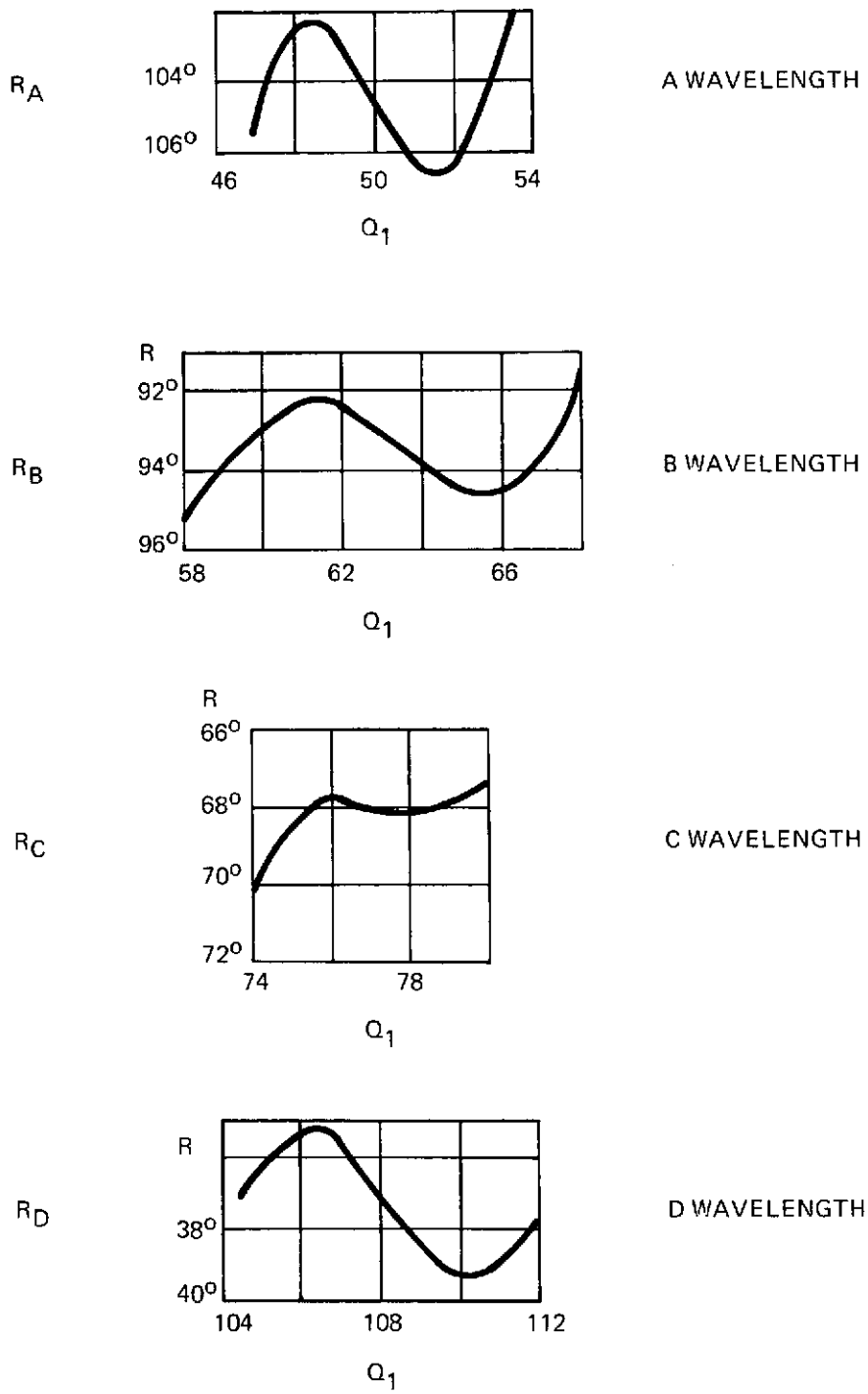

Figure 3 - Variation of R dial reading with Q setting.

Substituting these values into equation (35) together with previously evaluated terms, and using $\mu = 1.15$ for X_{AD}:

$$\Delta X_{AD} = .9923 \Delta Q_1 . \tag{39}$$

Using $\Delta Q_1 = 0.4$, the maximum allowable in the routine maintenance tests, results in

$$\Delta X_{AD} = .001 . \tag{40}$$

Adjustment of the Electronics: Because the instrument is basically a null-meter, calibration of the electronics in the sense of determining an input-output relationship is not necessary. The electronics must be periodically tested to determine that the sensitivity is adequate to enable the operator to find the correct null position, and that the commutator mechanism is correctly rectifying the alternating current amplifier output.

Relative Calibration of the Optical Filter Wedge: The relative calibration of the optical wedge consists of determining the tabular function which relates R-dial readings to logarithmic ratios of the two wavelength beam intensities, within an arbitrary constant. That is to say, relative calibration determines values of R vs $L_\lambda = \log(I_\lambda/I_\lambda') + K$, where the I_λ's represents the intensities of the two beams in a wavelength pair, and K is an arbitrary constant, determining the origin of the calibration curve. The constant K drops out when the extra-terrestrial constant $L_{o\lambda}$ is subtracted from L_λ to determine N_λ. The determination of $L_{o\lambda}$ is known as "absolute calibration," and is discussed below.

"Absolute Calibration" of the Spectrophotometer: The "absolute calibration" of the Dobson instrument, as now carried out, consists of finding the extra-terrestrial constant $L_{o\lambda}$, the value of $(\log (I_o/I_o')+K)$ for the sun's radiation outside the earth's atmosphere. Referring back to equation (10) and adding K to both sides:

$$\begin{aligned} \log(I/I') + K = \log(I_o/I_o') + K \\ - (\alpha-\alpha') X\mu - (\beta-\beta')m \\ - (\delta-\delta') \sec Z , \end{aligned} \tag{41}$$

$$L_\lambda = L_{o\lambda} - (\alpha-\alpha')\ X\mu\ -\ (\beta-\beta')m\ -\ (\delta-\delta')\sec Z. \qquad (42)$$

The assumption is made that there is no variation in the amount of ozone over a one-day interval. Then all of the factors appearing in equation (42) are constant, except L_λ, μ, m and sec Z , and all are assumed known except $L_{o\lambda}$ and X . Rewriting (42) in the form

$$(L_\lambda + (\beta-\beta')m + (\delta-\delta')\sec Z) = L_{o\lambda} - (\alpha-\alpha)\ X\mu, \qquad (43)$$

shows that if the left hand side is evaluated for a number of measurements with different values of μ but with constant X , and the results plotted against μ , the plot will be a straight line with slope equal to $-(\alpha-\alpha')X$ and intercept, at $\mu = 0$, of $L_{o\lambda}$. The absolute calibration procedure in use performs the calculations somewhat differently, but the underlying assumption is the same, that the total ozone remains constant over a one-half day interval. The measurements are made on a number of days, and an averaging process is used on the results. The resulting value of $L_{o\lambda}$ is subtracted from the L_λ values in the relative calibration tables, to provide tables of N_λ vs R

$$N_\lambda = L_\lambda - L_{o\lambda}. \qquad (44)$$

The error in the values determined by the process can not be established by analytical means, since it depends on the assumption of no mean variation in X during the daylight hours.

In practice, the procedure described above is not carried out for every spectrophotometer. One instrument located at Boulder, Colorado is maintained as a standard, and the above calibration is repeated periodically. The absolute calibration of this instrument is transferred to other instruments by one of two ways; either by setting the two instruments side by side, making simultaneous measurements of ozone, and inter-comparing the results, or by using standard lamps to transfer the calibration from one instrument to the other.

Errors in Data Due to Errors in Optical Wedge Calibration: The errors in X_{AD} caused by calibration errors can be evaluated in terms of errors in N_A and N_D.

The error equation is

$$\Delta X_{AD} = 0.007205(\Delta N_A - \Delta N_D)/\mu . \tag{45}$$

Using 1.0, the extreme error in N_A or N_D allowed by the calibration checks, as the two-sigma value, and setting $\mu = 1.15$, the error in ozone data, caused by calibration errors with this distribution, is

$$\Delta X_{AD} = .003. \tag{46}$$

Variations in Extra-Terrestrial Constant: The extra-terrestrial constant, $L_{o\lambda}$, may vary due to variations in the solar spectrum. The resulting error in reduced data from AD wavelength pair measurements will be

$$\Delta X_{AD} = .7205(\delta L_{oD} - \delta L_{oA})/100_{\mu}. \tag{47}$$

Setting $\mu = 1.15$, and taking the square root of the sum of the squares of the error caused by δL_{oD} and δL_{oA},

$$\delta X_{AD} = 0.00886\ \delta L_o. \tag{48}$$

If the variation in intensity ration I_o/I_o' is taken as 1% of the nominal value, the variation in $\log_{10}(I_o/I_o')$ is .00434 and the variation in L_o is 0.434, yielding

$$\delta X_{AD} = .00384$$

for each 1% of variation in I_o/I_o'.

Variations in Ozone Absorption Coefficient with Temperature: The ozone absorption coefficient α, is based on the assumption that the temperature in the region of ozone absorption is -44°C. Since the absorption coefficient of ozone is temperature dependent (see Table 3),

the seasonal and latitudinal variations of the temperature profile vs. altitude will affect the total absorption and cause an error in reduction. The weighted mean of the temperature over the altitudes of ozone concentration can vary as much as 5° due to seasonal effects. From equation (15) the computed value of ozone is proportional to the inverse of $\alpha_A - \alpha'_A - \alpha_D + \alpha'_D$, and from Table 3, a variation of 5°K can cause 3% change in the quantity, thus a 3% error in reduced total ozone.

Particulate Scattering Effect (Single Scattering Only): The assumption is made that the effects of particulate scattering are only slightly wavelength dependent, so that, for example:

$$(\delta - \delta')_A - (\delta - \delta')_D = 0.$$

The error in ozone data caused by this assumption is strongly dependent on the actual functional relationship between the scattering coefficient and the wavelength, and cannot be evaluated until experimental data on the scattering functions are available.

Error in Determination of Extra-Terrestrial Constant. - The extra-terrestrial constant is derived based on two assumptions:

a) First, that the mean variation of ozone during daylight hours is zero.

b) Second, that the effective or apparent ozone absorption coefficient, including the extinction due to scattering by molecules and aerosols, is a constant for a large range of zenith angles.

Electrochemical Concentration Cell Ozonesonde

System Description. - The Electrochemical Concentration Cell (ECC) Ozonesonde, as described in Reference 6, is a device designed to be flown in conjunction with, and on the same balloon as, a standard National Weather Service meteorological radiosonde. The sensing unit of the ozonesonde is an iodine/iodide redox electrode concentration cell composed of two platinum electrodes immersed in potassium iodide solutions of different concentrations in the cathode and anode chambers. When the circuit is closed, the cell

quickly attains equilibrium and no current flows. If air containing ozone is introduced into the cathode chamber, a chemical reaction takes place, creating iodine (I_2), which the cell converts back to potassium iodide, causing a current of two electrons to flow for each molecule of ozone introduced, until the ozone is destroyed and equilibrium is attained.

In the ozonesonde, a continuous stream of ambient air is bubbled through the sensor by a constant volume pump, causing a current to flow which is proportional to the ozone concentration. The pump motor also drives a data sequencing switch which causes the ozonesonde data to periodically over-ride the standard meteorological transmission of the radiosonde.

An electronic coupler converts the ozone sensor output into a resistance whose magnitude is sensed by the radiosonde circuitry. The radiosonde transmits at a frequency of 1680 MHz through a blocking oscillator which interrupts the transmission in a square wave pattern with frequency ranging from 0 to 190 Hz. The data sequencing switch causes data to be transmitted in a two minute sequence, with six ozone readings, an ozone zero reading, an ozone calibrate reading and an ozone sensor temperature reading transmitted in each cycle. The ozonesonde readings occupy one fourth of the cycle, and the standard meteorological readings of air pressure, air temperature and humidity of the radiosonde occupy the other three fourths. At present the data are recorded on strip charts and reduced manually.

Operating Procedures. -

Preflight Preparation: Two to ten days prior to use, the ozonesonde is "conditioned" by passing air containing a high proportion of ozone through the sonde for about 1/2 hours, with no sensing solution in the anode and cathode chambers. This serves to deactivate the surfaces in the unit so that no reaction will occur to destroy ozone during operations. At the same time, the ozonesonde output leads are connected to a test unit and the potentiometer in the electronic coupler adjusted. After conditioning, an ozone destruction filter is attached to the sonde air intake tube and the sonde anode and cathode chambers are changed with electrolyte.

The sonde is conditioned for 20 minutes with ozone-free air, using an ozone destruct filter on the air intake, and the time, t , for the pump to transfer 100 ml. of air is measured and recorded for use in data reduction.

About one-half hour before release time the radiosonde base-line calibration is performed, then the ozonesonde is connected to the radiosonde, and the ozone destruct filter is attached to the air intake, and the radiosonde receiver adjusted so that the low reference signal falls at 95.0 chart ordinates, and the ozonesonde coupler potentiometer adjusted so that ozone zero signals occur at about 35.0 chart ordinates. A seven minute "zero adjust" recording of the ozonesonde output is obtained. The temperature of the ozonesonde box during the zero adjust is measured and recorded. All of the above is performed in an enclosed, protected area, free from air contamination. The instrument is then connected to the balloon train and released.

In Flight Operation: The sonde is carried by a balloon of capacity allowing a rise rate of about 300 meters/minute. During the flight, the frequency control knob on the radiosonde receiver is adjusted to maintain the low reference signal at 95.0 chart ordinates.

Data Reduction. -

Theory of Measurement: Exact analysis of the electrochemical reactions within the ozone sensing cell will not be given, because, to quote from Reference 7: "A rigorous analysis of the characteristics of the real cell is difficult, if not impossible, to perform not only because of its complexity but because the cell anode chamber contains electrolyte saturated with potassium iodide for which ionic activities cannot be computed." Kohmyr, in Reference 7. concludes that "The current flowing in the external circuit is ... directly related to the rate of conversion of iodine to iodide, or iodide to iodine."

The proportion is very nearly two electrons for each molecule of iodine converted. When air containing ozone is bubbled through the cathode electrolyte, the reaction

$$2KI + O_3 + H_2O \rightarrow 2KOH + I_2 + O_2 \qquad (49)$$

takes place. The I_2 molecule is converted back to KI by the action of the cell, causing two electrons to flow in the external circuit for each molecule of ozone introduced.

The ozone concentration can be derived from the equation (Reference 6):

$$P_3 = 4.307 \times 10^{-3} \; I \; T_b \; t, \tag{50}$$

where

P_3 is the ozone partial pressure in micro-millibars,

I is the sensor current due to ozone in micro-ammperes,

T_b is the sonde box temperature in degrees Kelvin, and

t is the time in seconds taken by the pump to force 100 milliliters of air through the sensor.

It is observed that the cell puts out a background current, I_a, when pure ozone-free air is bubbled through it. The value of I_a is usually very low, and is observed during the pre-flight zero check procedure. The ozone current I used in Equation (50) is defined by

$$I = I_{obs} - I_a, \tag{51}$$

where I_{obs} is the cell current observed during ozone measurement.

Data Reduction Method:

a) The following traces are identified on the chart record, a sample of which is shown in Figure 4, where

Z = ozone zero,
C = ozone calibration,
Oz = ozone measurement, and
T_b = box temperature.

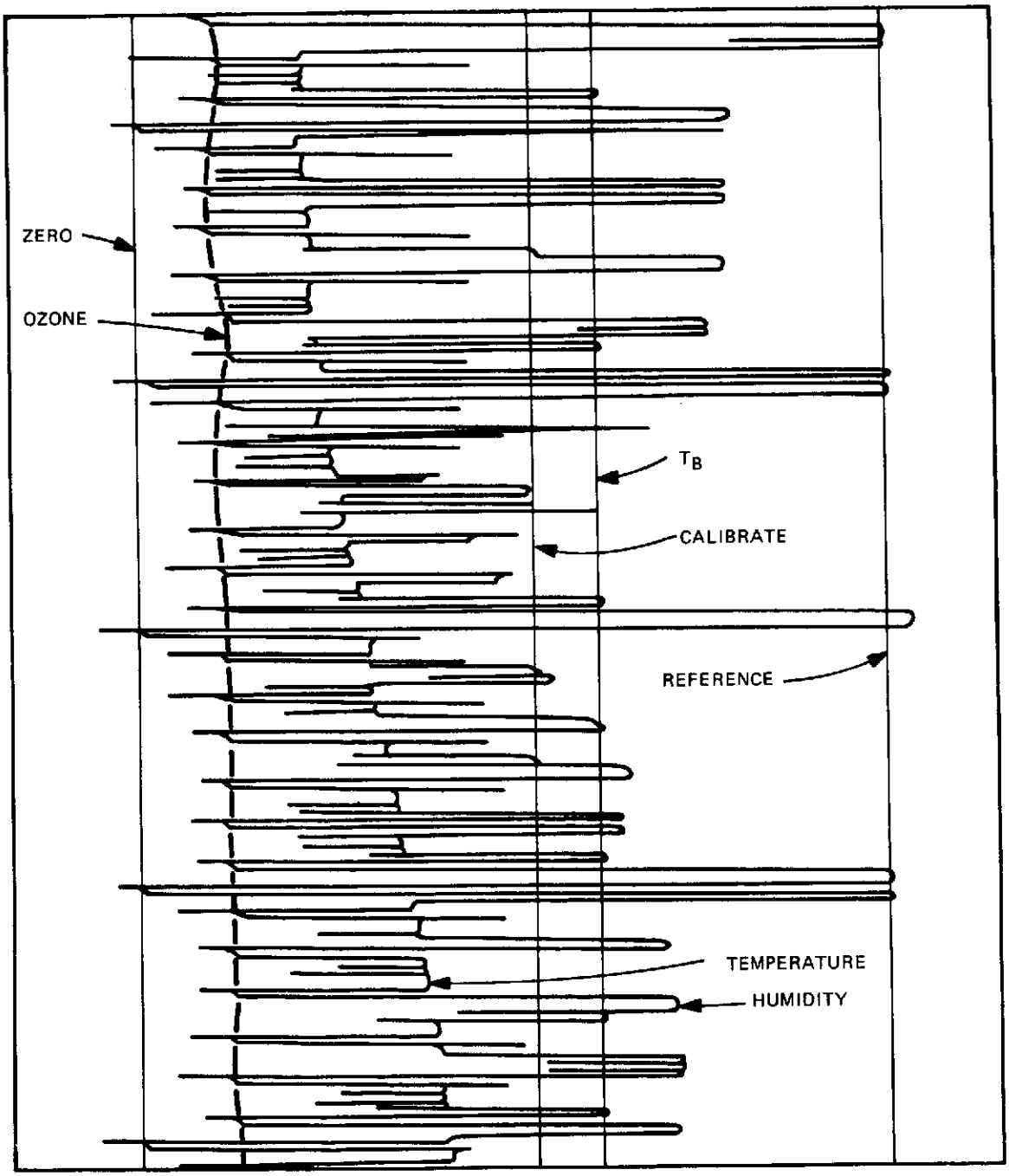

Figure 4 - Sample ozonesonde record.

The segments of each trace are connected to form continuous lines for Z, C, Oz and T_b.

b) Levels to be measured are selected at points on the chart where a pressure measurement is made, that is, where the radiosonde commutator switches from temperature to humidity or reference measurement.

Measurement levels are selected at mandatory levels, that is, at surface pressure, 1000, 700, 500, 300, 250, 200, 150, 100, 70, 50, 30, 20, 10, 7, 5, 3 millibars, at the tropopause levels, at levels of prominent maximum and minimum of the Oz trace and at points which provide about 1 chart ordinate spacing between the other points selected.

c) Using an ozone scale, provided with the manual, Oz and C are measured with respect to the Z trace. The contact number on the radiosonde commutator, the temperature ordinate and the reading for box temperature T_b are also read. I_a, the current due to ozone-free air alone, is read by measuring Oz and C in the zero adjust portion of the chart.

d) A scale value S from the above reading is computed by

$$S = 314 \frac{Oz}{C} . \qquad (52)$$

e) Current readings are obtained from values by using the tables or calibration curve (Figure 5) of current vs signal divisions, provided with the manual.

f) The readings of I_a are corrected for ambient pressure by a chart using Table 2 because the background current caused by ozone-free air is assumed to be proportional to the partial pressure of oxygen in the air.

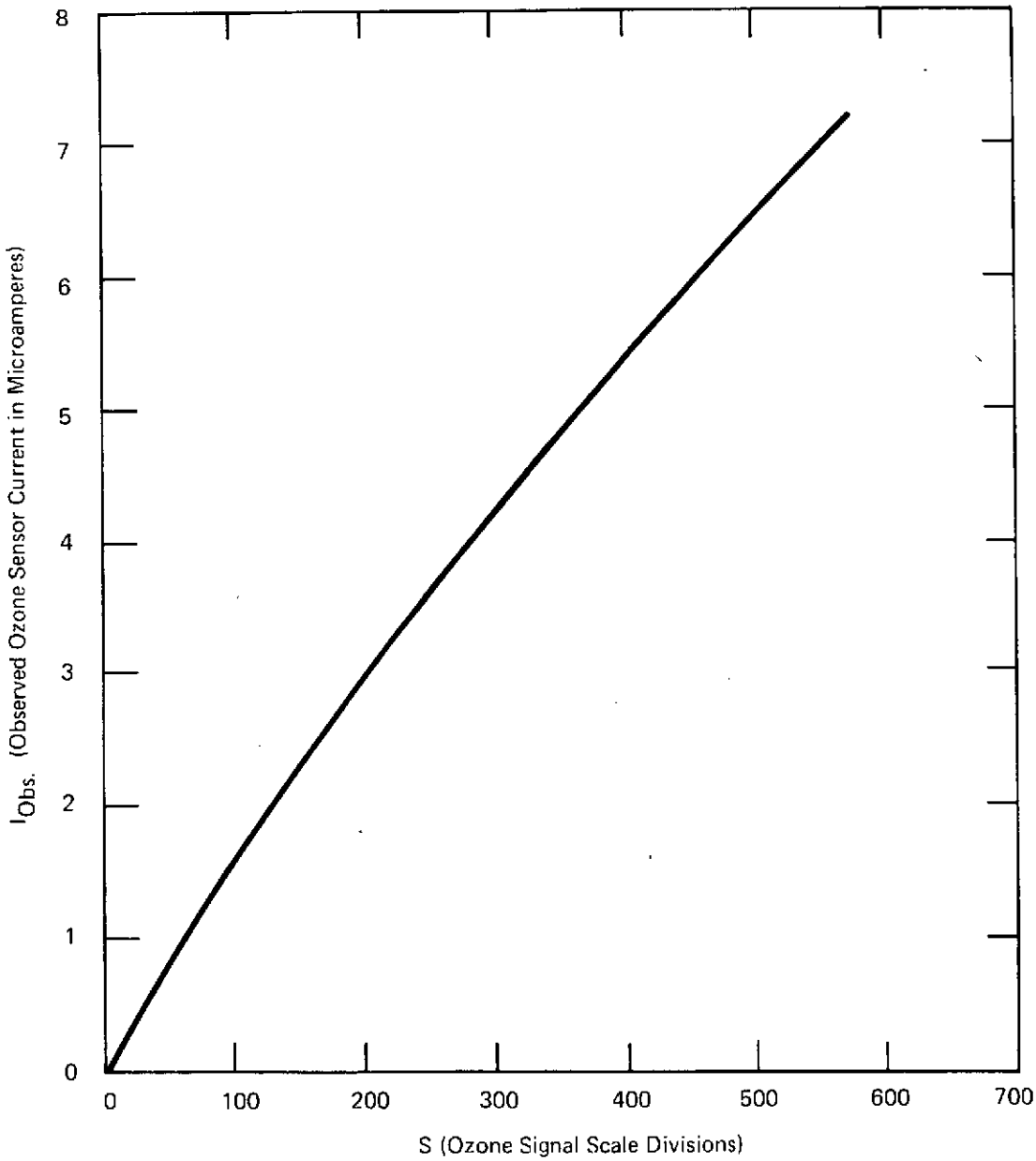

Figure 5 - Calibration curve for ECC ozonesonde models.

TABLE 2

Pressure Interval (mb)	VALUES OF i_a (μA) (1)	(2)	(3)	(4)	(5)	(6)	(7)	(8)	(9)	(10)
1070-951	0.55	0.50	0.45	0.40	0.35	0.30	0.25	0.20	0.15	0.10
950-830	.50	.45	.41	.36	.32	.27	.23	.18	.14	.09
829-711	.44	.40	.36	.32	.28	.24	.20	.16	.12	.08
710-596	.39	.35	.32	.28	.25	.21	.18	.14	.11	.07
595-485	.33	.30	.27	.24	.31	.18	.15	.12	.09	.06
484-379	.28	.25	.23	.20	.18	.15	.13	.10	.08	.05
378-279	.22	.20	.18	.16	.14	.12	.10	.08	.06	.04
278-191	.17	.15	.14	.12	.11	.09	.08	.06	.05	.03
190-114	.11	.10	.09	.08	.07	.06	.05	.04	.03	.02
113-57	.06	.05	.05	.04	.04	.03	.03	.02	.02	.01

g) The box temperature T_b is reduced, using the Radiosonde Temperature Evaluation to convert chart readings to temperature.

h) The ozone partial pressure is computed by

$$P_3 = 4.307 \times 10^{-3} (I_{obs} - I_a) T_b t. \qquad (53)$$

i) The ozone values are corrected for the variation of pump efficiency with pressure, using the curve in Figure 6, by multiplying P_3 from equation (53) by the partial pressure correction factor from the curve.

Error Analysis. - As with the error analysis of the Dobson instrument, this analysis will examine four areas:

a) The observer error in reducing the traces on the T.M. charts.

b) The propagation of the above error through the data reduction equations.

c) The errors in the data caused by instrument calibration and adjustment errors.

d) The errors in the data caused by assumptions in the derivation of the reduced equations.

Measurement Errors: The basic measurements to be considered are the measurement of the values Oz (ozone measurement) and C (calibration measurement) with respect to the Z (ozone zero) trace; the determination of T_b (box temperature); and the determination of pumping time t.

In the measurement of Oz and C with respect to Z there are two sources of error: the determination of where to draw the three traces connecting the contact points on the chart (Figure 4), and the measurement of the distance between the lines, in terms of ozone scale units. Measurement errors of this type are difficult to assess analytically without carefully controlled statistical experiments using trained observers to measure quantities of data from a variety of records. However, in the experience of the writer with graphical reduction techniques, the error to

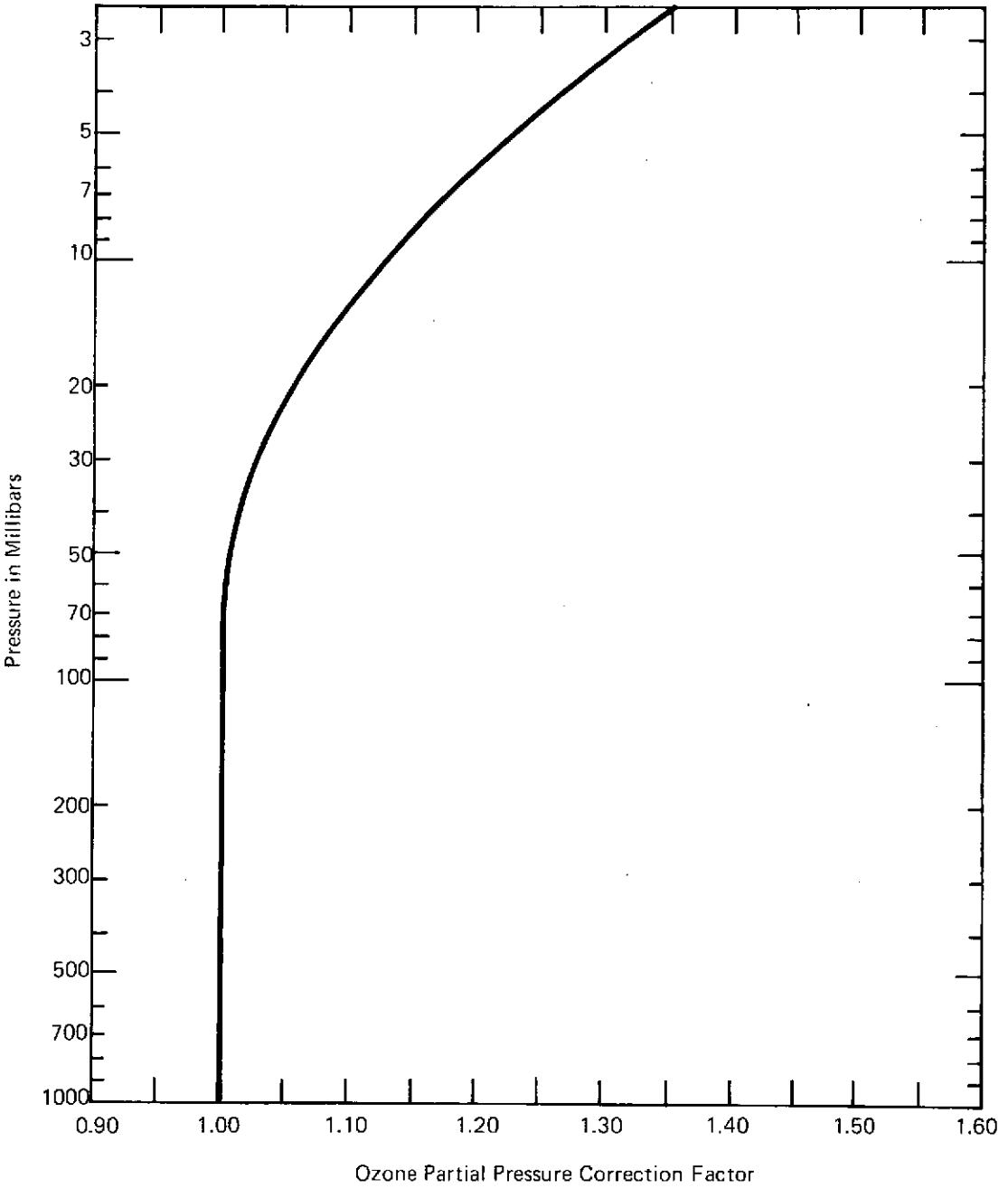

Figure 6 - Ozone partial pressure correction curve (corrections for decreasing pump air flow rate at reduced ambient pressure).

be expected is 0.1 to 0.2 chart units in drawing the connecting lines, and 0.1 chart units in measurement of the distance between lines. The ratio of chart units to ozone scale units is about 1 to 10. Allowing 1.5 ozone scale units for error of measurement of the distance between two lines, and taking the square root of the sum of the squares of the three errors, allows

$$\sigma_{oz} = \sigma_c = 2.3 \text{ scale units.} \tag{54}$$

The error in determination of box temperature T_b from the record, using standard radiosonde technique has been estimated at 0.5° C at lower altitudes, increasing to 2.0° C at the higher altitudes reached by the balloon (Reference 6).

The error in measurement of t, the time for the pump to force 100 ml. of air through the sonde, is estimated at 0.2 sec.

The estimates above are empirical, arrived at to some extent by intuitive judgement of graphical data reduction methods based on experience.

Error in Determining the Ozone Current: Repeating Equation (52), the ozone scale reading is obtained from:

$$S = 314 \frac{Oz}{C},$$

$$\Delta S = \frac{\partial S}{\partial Oz}\Delta Oz + \frac{\partial S}{\partial C}\Delta C, \tag{55}$$

$$\frac{\partial S}{\partial Oz} = \frac{314}{C}, \tag{56}$$

$$\frac{\partial S}{\partial C} = \frac{-314\ Oz}{C^2}. \tag{57}$$

Since the adjustment of the scale is such that $C \simeq 314$

$$\frac{\partial S}{\partial Oz} = 1, \tag{58}$$

$$\frac{\partial S}{\partial C} = \frac{-Oz}{C} = \frac{-S}{C}. \tag{59}$$

Since C corresponds to a current of 4.47 microamperes, which is nearly the maximum ozone current, let $S = C$ for a nominal value, and

$$\frac{\partial S}{\partial C} = -1. \tag{60}$$

Then allowing

$$\Delta Oz = \Delta C = 2.3$$

and using the root-sum-square to combine the two error effects to obtain the error of S due to measurement error,

$$\Delta S = \sqrt{2.3^2 + 2.3^2} = 3.2. \tag{61}$$

From the calibration curve in Figure 3

$$I \simeq \frac{4.47}{314} S, \tag{62}$$

and the error of I due to measurement error is

$$\Delta I = \frac{4.47}{314} \Delta S = .045. \tag{63}$$

Error in Determining P_3: To repeat equation (53):

$$P_3 = 4.307 \times 10^{-3} (I_{obs} - I_a) T_b t.$$

The error in P_3 is

$$\Delta P_3 = \frac{\partial P_3}{\partial I_{obs}} \Delta I_{obs} + \frac{\partial P_3}{\partial I_a} \Delta Ia + \frac{\partial P_3}{\partial T_b} \Delta T_b + \frac{\partial P_3}{\partial t} \Delta t. \quad (64)$$

Nominal values for the terms in Equation (53) are:

$$I_{obs} = 5.5 \ \mu a, \quad (65)$$

$$I_a = 0.5 \ \mu a, \quad (66)$$

$$T_b = 300°K, \quad (67)$$

$$t = 30 \text{ sec}. \quad (68)$$

Taking the indicated partials of equation (53) and substituting the nominal values yields:

$$\frac{\partial P_3}{\partial I_{obs}} = 38.8, \quad (69)$$

$$\frac{\partial P_3}{\partial I_a} = 38.8, \quad (70)$$

$$\frac{\partial P_3}{\partial T_b} = .646, \quad (71)$$

$$\frac{\partial P_3}{\partial t} = 6.46. \quad (72)$$

The root-sum-square error caused by the combined effects of measurement is

$$\Delta P_3 = 3.05 \text{ μmb.} \tag{73}$$

Using the nominal values,

$$P_3 = 194 \text{ μmb,} \tag{74}$$

so that the error in P_3 due to measurement error is of the order of 1.5% of the measured value.

Pumping Rate Variations: The curve of pump efficiency vs pressure (Figure 6) was arrived at experimentally under laboratory conditions. Variations in the pump efficiency factor of up to 5% at 10 mb and 15% at 3 mb can be expected (Reference 6). Below 70 mb the correction, hence the error, are presumed negligible. Since the ozone partial pressure at 10 mb is of the order of 50 μmb the magnitude of the error due to uncertainty in pump efficiency is

$$\Delta P_3 \simeq 2 \text{ μmb,} \tag{75}$$

The pumping rate varies not only with pressure, as shown in Figure 6, but with pump temperature. According to Reference 6, "the air-flow-rate vs temperature of the Teflon gas sampling pump has been experimentally determined to be about 0.065 percent/°C."

Experimental data show that between sea level and 50 mb the pump temperature drops about 16°F, causing a air-flow-rate change of 1%. At about 50 mb, the ozone partial pressure reaches a maximum of about 200 μmb, so that the maximum error due to pump temperature change is

$$\Delta P_3 = 2 \text{ μmb.} \tag{76}$$

Box Temperature Measurement: Experimental data (Reference 6) shows that the T_b sensor records a temperature which is about 6°C lower than the actual pump temperature, because of friction and enthalpy loss heating of the pump. This difference has been approximately corrected for by adjusting the calibration curve (Figure 3). The error in this correction is certainly

less than the maximum error allowed above in reduction of T_b, and already accounted for in the measurement error effects.

Changes in Electronic Coupler Gain and Zero Levels: The in-flight calibration, consisting of the "cal" and "zero" signals transmitted in every two-minute cycle of the sequencing switch, allows electronic coupler gain and scale zero effects, along with any drifts in the radiosonde telemetry system to be compensated for in the data reduction procedure. Measurement of Oz and C traces with respect to the Z trace, and use of equation (52) to compute S, accomplish this compensation.

Cell Chemistry: To quote from Reference 6, "The ECC ozone sensor is an absolute device in that if we assume that each ozone molecule entering the sensor causes a current flow of two electrons in the sensor external circuit, then no auxilliary instrument need be used to calibrate the sensor. Considerable controversy exists, however, even now in the formal literature about the stoichiometry of the oxidation of iodine by ozone in KI solutions. Ingols et al. (1959), for example, found that twice as much iodine was liberated by ozone in a KI solution of pH2 as compared with iodine liberated in a solution of pH9. Byers and Saltzman (1959) assumed that at pH7 the ratio of iodine molecules to ozone molecules was 1:1. More recently, Boyd et al. (1970) has argued that the stoichiometry of the reaction of ozone with a neutral potassium iodide solution is such that one molecule of ozone liberates 1.53 molecules of iodine."

Calibration tests of ECC sensors against standard ozone generators indicated that the sensors agreed within $\pm$ 5 percent with the generator calibration curves (Reference 6). Other data on instrumental intercomparisons with Dobson Ozone Spectrophotometers is given in a later section of this report.

Background Current. - The assumption that the background current is caused only by the atmospheric oxygen, and is proportional to the partial pressure of oxygen, is not completely verified. Trace pollutants, passing the ozone destruct filter, could cause a background current not proportional to atmospheric oxygen. If the error in I_a for this cause is 0.05 μa, the error in ozone partial pressure, using equation (70) is

$$\Delta P_3 = 2 \text{ μmb.} \qquad (77)$$

or 1% of the nominal measurement given by equation (74)

Sensor Response Time: Test data (Reference 6) shows that the sensor exponential response time is of the order of 20 seconds. This means that a step change in ozone concentration, at a rise rate of 300 meters/min. will be detected with 33% error in 100 meters and 5% error in 300 meters.

Ozone Distribution Above: In the derivation of total ozone from ozonesonde observations by integration of the partial pressure curve, the assumption is made that the ozone mixing ratio is constant above the height of balloon burst. If the assumption is correct, and if the balloon reaches the 30 kilometer level, the errors in this calculation are less than 1%. If the assumption is not correct, errors of up to 5% might be possible. Some suggestions have been made that a secondary maximum of ozone concentration occurs at about 40 kilometers, and some evidence for existance of the maximum was shown on two records taken by Randhawa at White Sands. Using rocket-borne ozonesondes, however, Randhawa, in other measurements, and other experiments, have found no evidence of such a peak (References 9-13). If such a peak exists, then the error in total ozone computation may be as great as 5 to 10%.

Sample Dual Instrument Sounding: The ozonogram showing the two ozone profiles from a carefully controlled dual instrument sounding is shown in Figure 7. Reference 6 contains a discussion of the test. The profiles show the following points of interest:

a) The fine detail of the profiles in the region of 200 mb to 50 mb, (12 km. to 21 km.), is well reproduced on both traces. The differences in partial pressure readings of the two instruments are less than 5 μmb at the 100 mb level and increase to about 10 μmb at the 45 mb level.

b) Above 22 km, the two traces both follow a curve which approximates a curve of constant mixing ratio, but the two readings disagree by about 5 to 10%.

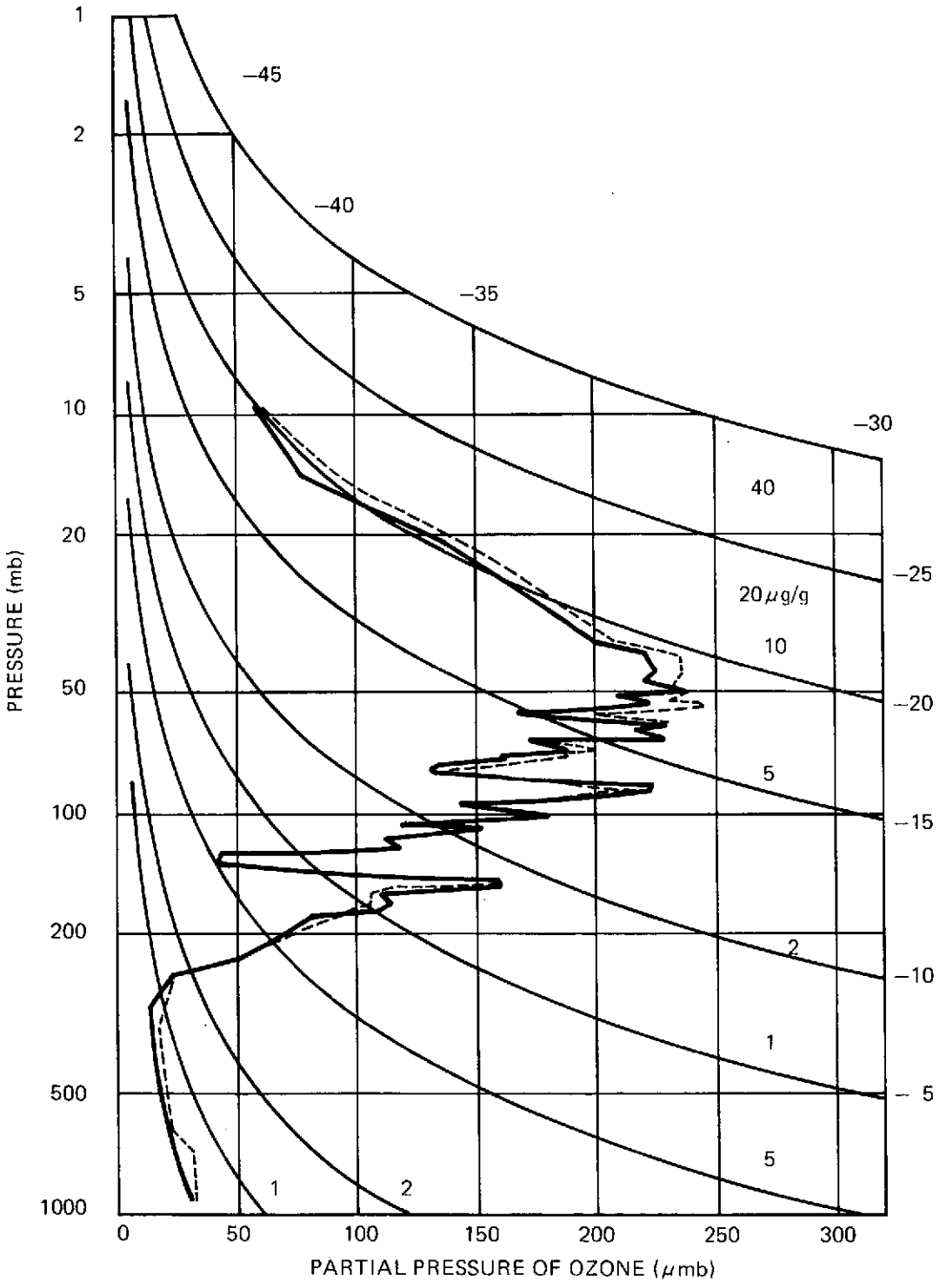

Figure 7 - Dual-instrument ozone sounding.

MONTE CARLO SIMULATION

A Monte Carlo Model of the Dobson ozone estimation scheme has been assembled and tested. The model can compute the effect of multiple scattered sunlight on the atmospheric ozone density inferred from Dobson Spectrophotometer measurements. The program possesses a unique feature. Unlike the Monte Carlo simulations of Kattawar and Plass[14] and Collins and Wells[15] the present method does not use direct sampling of photons. Rather, it samples hypothetical photons from each scattering on a probability basis. This technique has two important advantages:

1) The variance is considerably reduced,

2) We can sample sky radiance in exactly specified directions and do not have to use averaging techniques.

Polarization is fully treated by applying the Mueller algebra to the Stokes vector associated with each photon. The program can model ten receiver configurations simultaneously, including direct sun observations from ground level, zenith sky observations from ground level and nadir observations from satellite altitudes for any solar zenith angle less than 60°. The constraint on the solar zenith angle is imposed by the plane-parallel atmosphere assumed in the Monte Carlo simulation. Other receivers at any altitude and with any orientation can also be specified by the user. Thus, as a byproduct of the Dobson computations we can investigate the effect of multiple scattering on observations made in or above the atmosphere.

Analysis of the Dobson Spectrophotometer Experiment

In the direct Sun mode the Dobson Spectrophotometer measures the solar intensities at pairs of specified wavelengths. Normally, three wavelength pairs are employed and the ratios of the intensities employed to estimate the total ozone contained in a vertical column of the atmosphere. The result for total ozone is usually expressed in units of atm.-cms. which is the height in centimeters of a column containing all of the ozone above it reduced to standard temperature and pressure.

For a given line pair we define the parameter N_λ as:

$$N_\lambda = \log_{10}\left(\frac{I_o}{I_o'}\right) - \log_{10}\left(\frac{I}{I'}\right) \tag{78}$$

where

I_o, I_o' are the intensities entering the top of the atmosphere, and

I, I' are the observed intensities at the bottom.

The prime indicates the upper wavelength of the line pair. Although the contribution of molecular scattering to the attenuation of the sun's rays can be calculated fairly easily the contribution of the atmospheric aerosols can vary from day to day. An attempt is therefore made to eliminate this component by subtracting the results of two experiments performed with different wavelength pairs.

The final result of the experiment appears as given in equations (17) and (18).

$$X_{AD} = 0.7205\ (N_A - N_D)/\mu - 0.009,$$

$$X_{CD} = 2.037\ (N_C - N_D)/\mu - 0.012.$$

where the subscripts refer to the A, C and D line pairs respectively and μ is a parameter relating the slant path length through the ozone layer to its vertical height. For small zenith angles, Z, (say less than 60°) there is little error in taking μ to be sec Z.

Now the values of N_A, N_C and N_D appear to depend on the values of $\frac{I_o}{I'_o}$ for the three cases. These ratios are normally inferred by observing the sun over a fairly wide range of zenith angles or air masses and interpolating to zero air mass. It is unnecessary, however, to use the correct values of $\frac{I_o}{I'_o}$ in the simulation in order to estimate the effect of scattered radiation on the ozone estimation. This is because the scattered intensity for any given receiver field of view and atmospheric characteristics is always directly proportional to the incident intensity as is the attenuated direct sunlight. Thus, the values of N_A, N_C and N_D for a given configuration are independent of the ratio of the incident intensities even when the scattering of radiation into the receiver is important. In our simulations we artificially set $I_o = I'_o$ for each wavelength pair so that N_λ becomes simply $\log \frac{I'}{I}$.

In our calculations we know the true value of the total ozone, X, as a part of our model. Thus we can vary the field of view and see how much error is introduced into the estimation by scattered radiation and the differential attenuations of molecular and acrosol scatterers.

It should be noted that since in our work we assume plane parallel boundaries for the atmosphere rather than spherical boundaries, the replacement of μ by sec Z is mandatory. Nevertheless, it must be remembered that the final results cannot be trusted for large values of Z, greater than about 60°.

The Atmospheric Model

The computer program employed in this study accepts as data any atmospheric model the user wishes to investigate. Nevertheless in order to limit the amount of computer time we restricted our considerations to a U.S. Standard atmosphere in the mid-latitude range.

The temperature model employed was the July model from the U.S. Standard Atmosphere[17] and is presented in Figure 8. The densities of the molecular scatterers were taken principally from Champion's atmospheric model[22] which represents mean conditions throughout the year for latitudes near 30 degrees and altitudes above 30 kms. Below 30 kms. we used an average of Cole and Kantor's 30 degree latitude summer and winter atmospheres[23] to provide a smooth fit between Champion's densities and those of the U.S. Standard Atmosphere[17] which were used exclusively below 10 kms. The model densities employed for ozone and the other molecular components are graphed separately in Figure 9.

For the aerosol density we employed the Elterman model[16] as illustrated in Figure 10. The size distribution was assumed to be of the Junge type, i.e., the number of particles with diameters in the range D to D + dD was

$$\begin{aligned} n(D)dD &= (\nu-1)D_o^{\nu-1} D^{-\nu} dD, \quad \text{for } D \geq D_o; \\ n(D)dD &= 0 \qquad\qquad\qquad , \quad \text{for } D < D_o. \end{aligned} \tag{79}$$

The parameters selected in this work were

$$D_o = 0.2\mu$$

and

$$\nu = 4.$$

The absorption cross-sections for ozone that were employed in this study are summarized in Table 1. For intermediate temperatures, linear interpolation was employed. It was assumed that the other components of the atmosphere were responsible for scattering only, the cross-section for each molecule being the Rayleigh cross-section which is also given in Table 3.

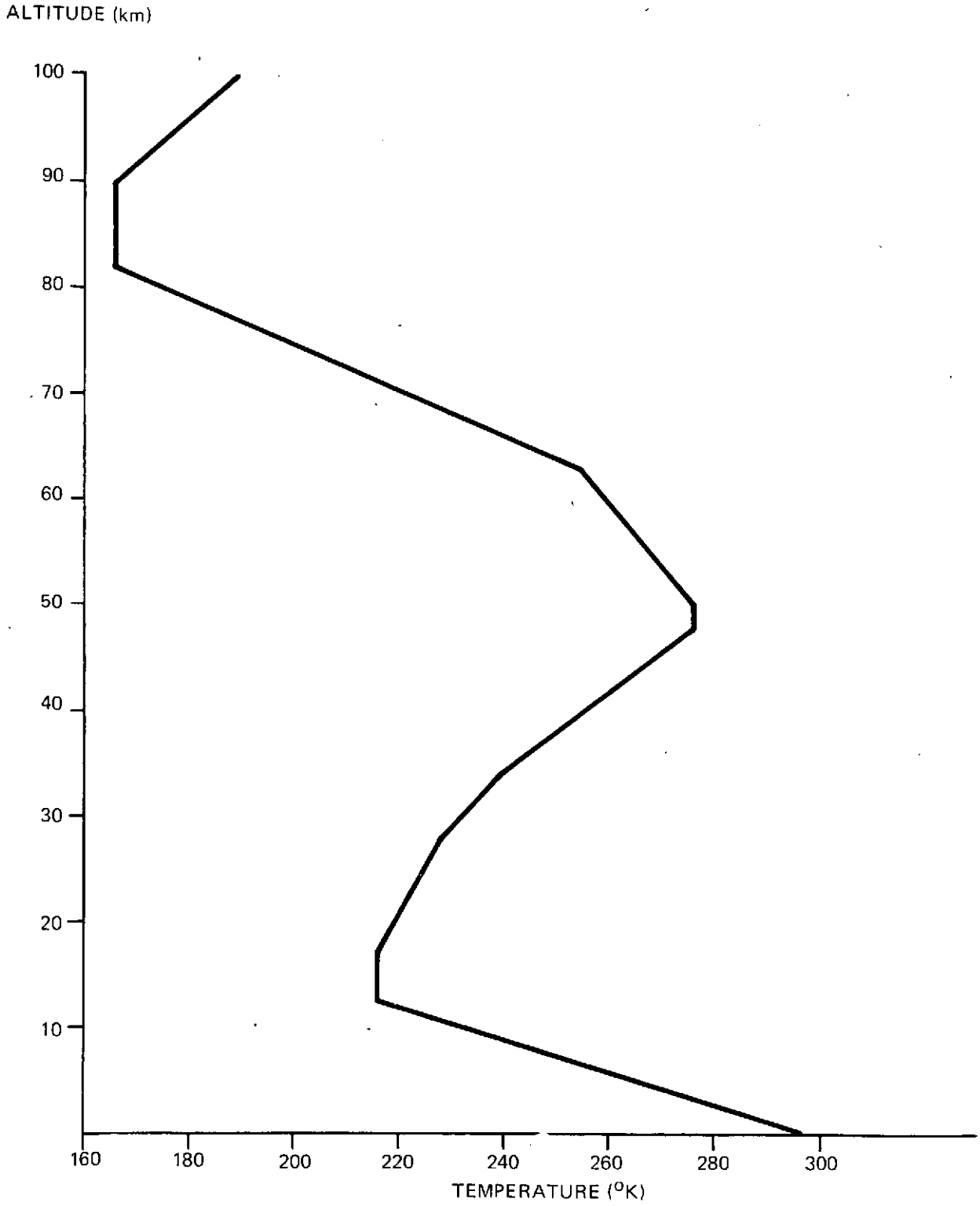

Figure 8 - Atmospheric temperature model.

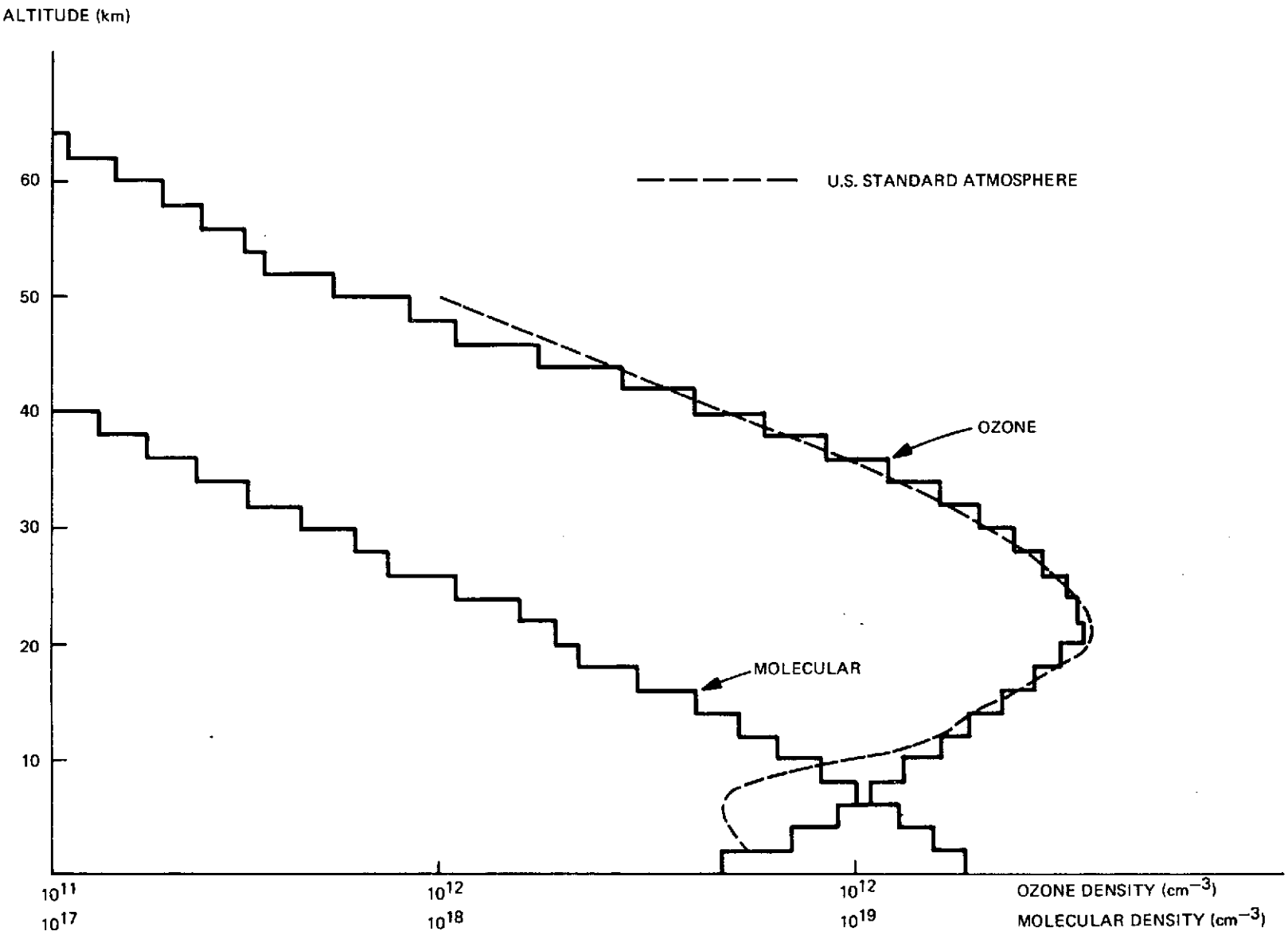

Figure 9 - Model Atmosphere: Molecular density and ozone density as function of altitude.

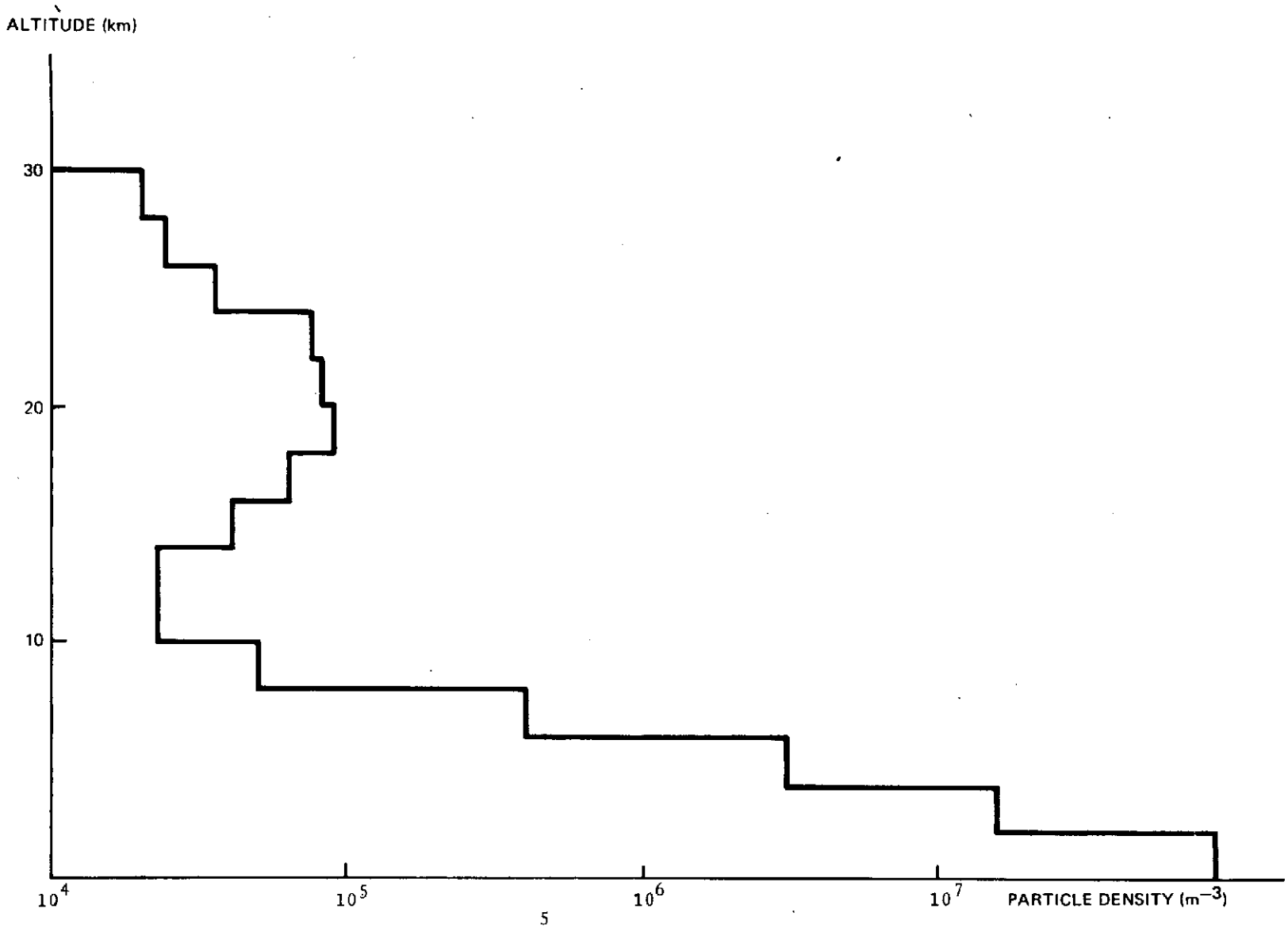

Figure 10 - Atmospheric model: Aerosol density as function of altitude.

The aerosol scattering properties were computed employing Mie scattering theory using a computer program supplied by Holland[18]. It was assumed that all particles were spherical with a complex index of refraction of (1.55 - 0i). Wavelength dependencies of the refractive index were neglected in this preliminary calculation so that the sole effect of changing wavelength was to alter the Mie particle size parameters, $\frac{\pi D}{\lambda}$.

The atmospheric model was stratified into 50 layers, each 2 kilometers thick. It was assumed that the density of each atmospheric component was uniform within each layer and equal to the average value within that layer. Thus the computer model was comprised of a series of step-like density profiles.

An important parameter influencing the overall radiative transfer characteristics of the atmosphere is the albedo for single scattering which is the fraction of the energy removed from the incident beam which reappears as scattered energy. The parameter is defined as:

$$\omega_0 = \frac{\beta_{SCA}}{\beta_{ABS} + \beta_{SCA}} = \frac{\beta_{SCA}}{\beta_{EXT}}$$ and can vary from a pure

scattering atmosphere ($\omega_0 = 1.0$) to pure absorption ($\omega_0 = 0$). The quantities β are volume scattering, absorption or extinction coefficients with dimensions of cm^2/cm^3 and are simply the products of the cross-sections for the constituents in each layer and the associated number of densities in the layer. In our model atmosphere only ozone absorbs and

$$\beta_{ABS}(Z) = \sigma_{ABS}(Z)\, n_{OZ}(Z).$$

The albedo for single scattering for our model is plotted as a function of altitude for the wavelength pairs of the A, C and D lines in Figure 11, 12 and 13, respectively.

TABLE 3. ABSORPTION CROSS-SECTIONS FOR OZONE AND RAYLEIGH SCATTERING WITH CROSS-SECTION (VALUES BASED ON $\log_e$)

		291°K	229°K	214°K	
		18°C	-44°C	-59°C	
DOBSON PAIRS	LINE λ (μ)	σ_{ABS} cm^2/molecule	σ_{ABS} cm^2/molecule	σ_{ABS} cm^2/molecule	σ_R cm^2/molecule
	.3055	1.757×10^{-19}	1.608×10^{-19}	1.582×10^{-19}	5.187×10^{-26}
"A" Lines	.3254	1.526×10^{-20}	1.254×10^{-20}	1.221×10^{-20}	3.964×10^{-26}
	.31145	8.634×10^{-20}	7.778×10^{-20}	7.554×10^{-20}	4.798×10^{-26}
"C" Lines	.3324	4.578×10^{-21}	3.461×10^{-21}	3.312×10^{-21}	3.621×10^{-26}
	.3176	3.745×10^{-20}	3.259×10^{-20}	3.223×10^{-20}	4.396×10^{-26}
"D" Lines	.3398	1.451×10^{-21}	1.116×10^{-21}	1.042×10^{-21}	3.297×10^{-26}

The Rayleigh scattering cross sections were calculated from the equation:

$$\sigma_R = \frac{3.321 \times 10^{-28}}{\lambda^{4.258}} \quad cm^2/\text{molecule where } \lambda \text{ , the wavelength is expressed in microns.}$$

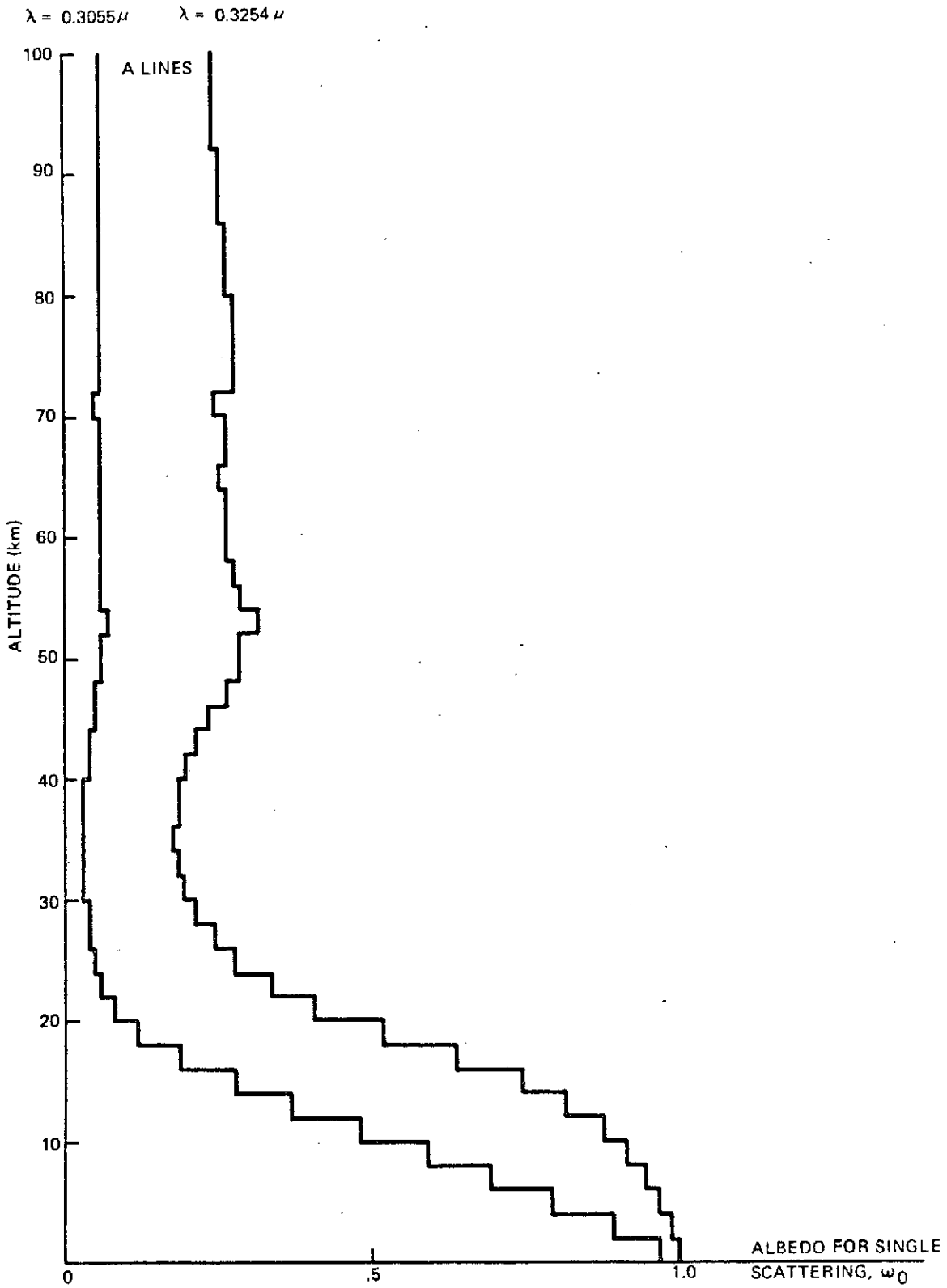

Figure 11 - Albedo for single scattering as function of altitude.

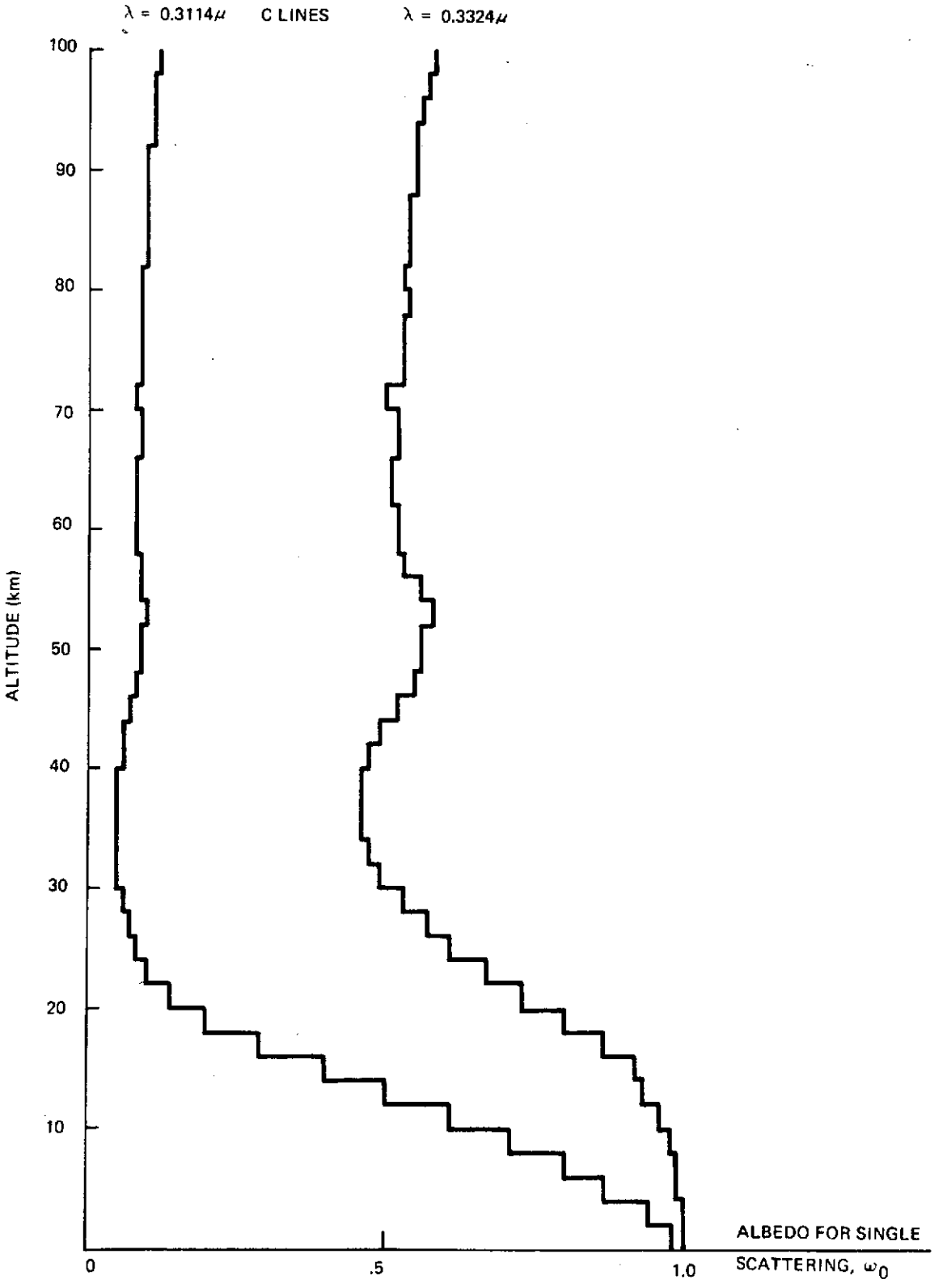

Figure 12 - Albedo for single scattering as function of altitude.

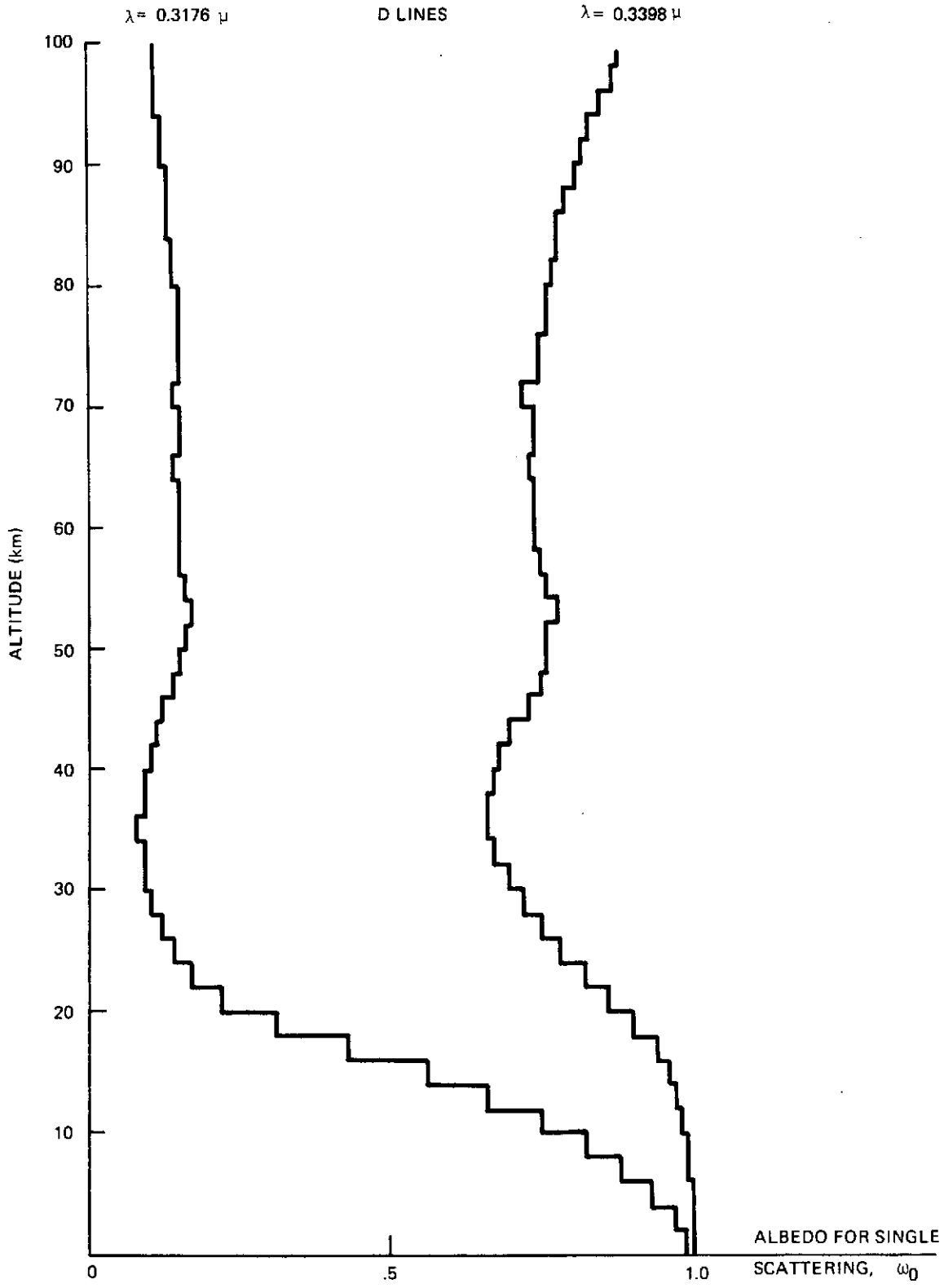

Figure 13 - Albedo for single scattering as function of altitude.

The total absorbing and scattering effects of the atmosphere can best be gauged by computing the optical thickness contributions of the atmospheric components. The optical thickness of each layer is defined as

$$\Delta\tau(Z_i) = [\beta_{ABS}\ (Z_i) + \beta_{SCA}\ (Z_i)]\ \Delta Z_i\ ,$$

$$\tau(Z) = \sum \Delta\tau\ (Z_i)\ .$$

These are presented in Table 4 for the six wavelengths of interest. It can be seen that all optical thickness contributions fall with increasing wavelength, the most rapid rate of change being for ozone and the least rapid being for the aerosol.

TABLE 4. ATMOSPHERIC OPTICAL THICKNESS CONTRIBUTIONS AS FUNCTION OF WAVELENGTH

LINES	WAVELENGTH (A.U.)	TOTAL	OZONE	AEROSOL	MOLECULAR
	3055	2.947	1.585	0.236	1.126
A					
	3254	1.224	0.124	0.239	0.861
	3114.5	2.037	0.767	0.232	1.038
C					
	3324	1.055	0.034	0.234	0.787
	3176	1.522	0.322	0.245	0.955
D					
	3398	0.957	0.011	0.229	0.717

Monte Carlo Simulation of Radiative Transfer Through the Atmosphere

A Monte Carlo simulation program has been written to investigate radiative transfer through a layered atmosphere. The details of the program are given in the Appendix and a schematic diagram of the simulation is given in Figure 14.

Essentially, the program computes the transport of photons entering the atmosphere from the Sun in terms of the optical thickness measured vertically from the ground plane. The optical depth of the slant path between encounters with atmospheric constituents is taken to be a random number with unit mean and an exponential distribution. For each encounter the particular layer of the atmosphere in which it occurs is determined by referencing the table of optical thickness as a function of altitude.

The next step is to determine whether the encounter is with an ozone molecule, another molecule or an aerosol particle. This is performed using a table of encounter probabilities for the constituents of the layer. The encounter probability is the normalized product of the constituent cross-section and its density in the layer. The importance of ω_0, the albedo for single scattering, is apparent in this context since the probability that the encounter is with an ozone molecule is simply $1-\omega_0$. A random number with a rectangular distribution between 0 and 1 is generated and this is cross-referenced with the probability table to select the appropriate constituent.

If the encounter is with an ozone molecule we assume the photon is absorbed and proceed to tracking a new incident photon. If the scatterer is another molecule we assume Rayleigh scattering whereas if the scatterer is an aerosol particle the scattering matrix elements are computed by averaging Mie theory results over the size distribution.

Three particle size distributions are allowed. These are:

$$\text{(a) Junge,} \quad n(D) = (\nu-1)\, D_0^{\nu-1}\, D^{-\nu} \quad \text{for } D \geq D_0, \qquad n(D) = 0 \quad \text{for } D < D_0; \tag{80}$$

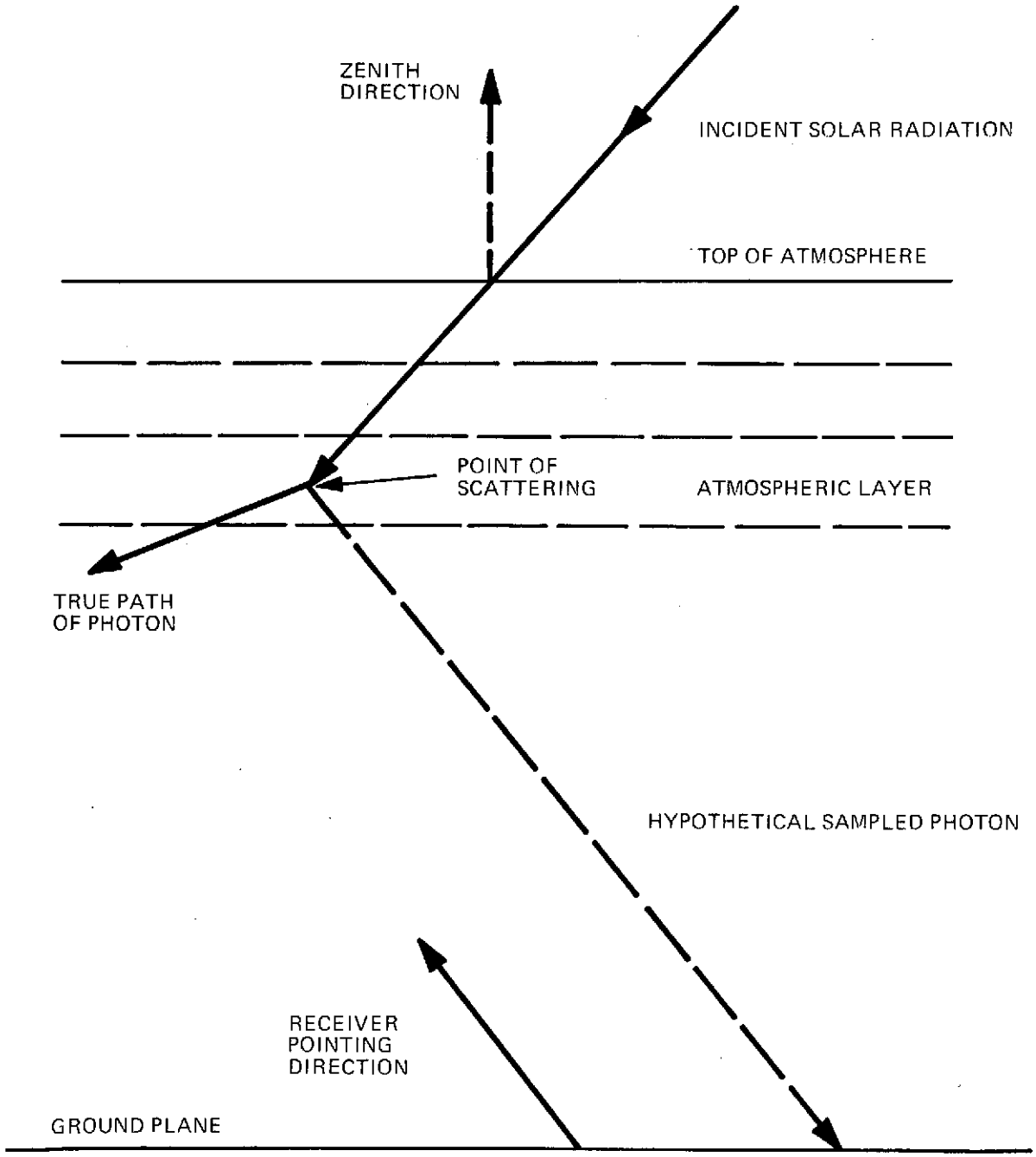

Figure 14 - Illustration of Monte Carlo method.

(b) Deirmendjiam, $$n(D) = \frac{\gamma\, b^{(\alpha+1)/\gamma}\, D^{\alpha}}{2^{\alpha+1}\ \Gamma\ \frac{\alpha+1}{\gamma}} \exp\left\{-b\ \left(\frac{D}{2}\right)^{\gamma}\right\}\ ; \qquad (81)$$

(c) Log-normal, $$n(D) = \frac{\delta}{(D-D_0)\ \sqrt{\pi}} \exp\left[-\delta^2 \left\{\ell n \left(\frac{D-D_0}{D_m-D_0}\right)\right\}^2\right]$$

$$\text{for } D \geq D_0, \qquad (82)$$

$$= 0 \text{ for } D < D_0.$$

Here $n(D)dD$ is the probability that the diameter, D, will lie in the range D to $D+dD$. D_0, ν, α, γ, b, δ and D_m are all constants dictating the particular shape of the distribution. The Deirmendjiam and log-normal distributions are more versatile than the Junge distribution, having three parameters rather than two. In fact, the Junge distribution can be fitted rather closely by either of the other two distributions with suitable parameters. All size distributions above are normalized distributions.

When the nature of the scatterer (other than ozone) has been established, we generate a series of hypothetical photons, one for each receiver pointing direction. (Most receivers are placed on the ground plane but this is not necessary.) At this point we compute the probability that a hypothetical photon would be scattered into unit solid angle of the field of view of each receiver and sample the Stokes vector which would be received if the event did occur weighted by the probability of occurrence.

After sampling has occurred we return to treat the transport of the real photon to the next scattering. If the real photon reaches the ground plane we assume Lambertian reflection, and provided the surface albedo is not zero, it is used to compute the Stokes vector of the reflected photon. The photon tracking mechanism is terminated in one or four ways:

1) An absorption occurs.

2) The photon leaves the top of the atmosphere.

3) At the ground plane if the surface albedo is zero.

4) The photon is found to have experienced more than a user specified upper limit to the number of scatterings.

The calculation at this point reverts to the next incident photon.

After a specified number of incident photons have been treated, we compute the average Stokes vector contribution for each receiver normalized to an incident flux of π photons per unit area normal to the incident beam. For the receiver pointing directly towards the sun we evaluate the total intensity due to direct and scattered light for a number of receiver fields of view.

Model Verification

Two sources of analytical results are available for the purposes of checking the computations. Dave, Sekera and Coulson[20] have computed the Stokes parameters for a pure Rayleigh atmosphere and Dave and Furukawa[21] have calculated the results for a realistic atmosphere including ozone for all orders of scattering.

In Figures 15 and 16 we present comparisons of the results obtained using a one layered version of the present program with those of Dave, Sekera and Coulson. The Stokes parameters I and Q are plotted as a function of the cosine of the zenith angle, μ', for an input flux of one photon per unit area with a Stokes vector of $(\pi,0,0,0)$. The value, π, was chosen so as to facilitate the comparison of the results with those of other authors. The cosine of the solar zenith angle in both cases was $\mu_0=0.6$. Since only 1000 incident photons were involved in the test, the agreement in the results is very satisfactory.

Examples of comparisons of the present results with those of Dave and Furukawa are given in Figures 17 and 18. The discrepancy in the intensity parameter can be attributed to the small difference in wavelengths and rapid change of the ozone absorption cross-section in this region. Overall, however, the agreement is perfectly acceptable. As expected, the polarization agreement was even better, since this term is not dependent on the ozone cross-section.

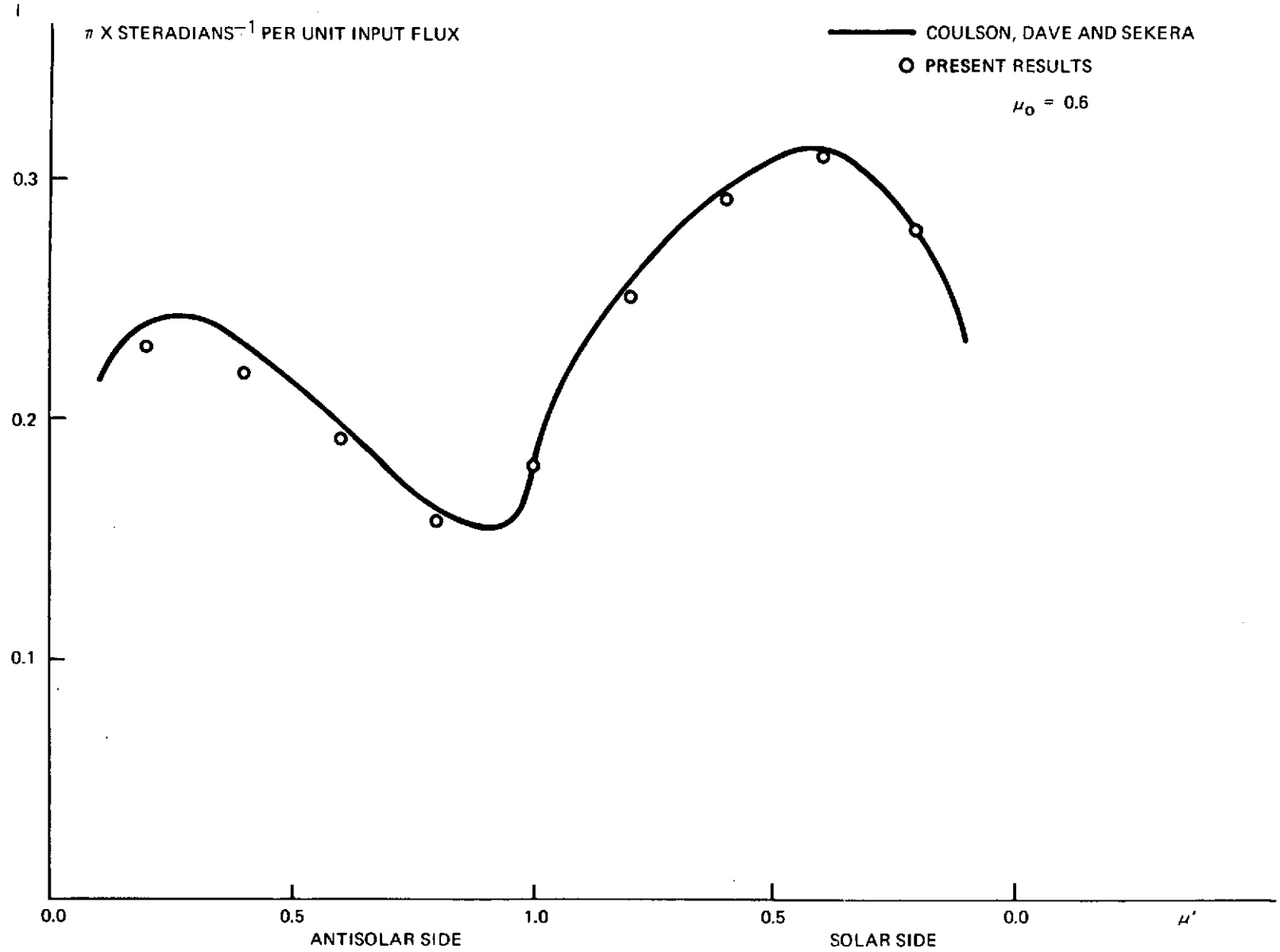

Figure 15 - Parameter, I, as function of zenith angle for optical thickness=1.

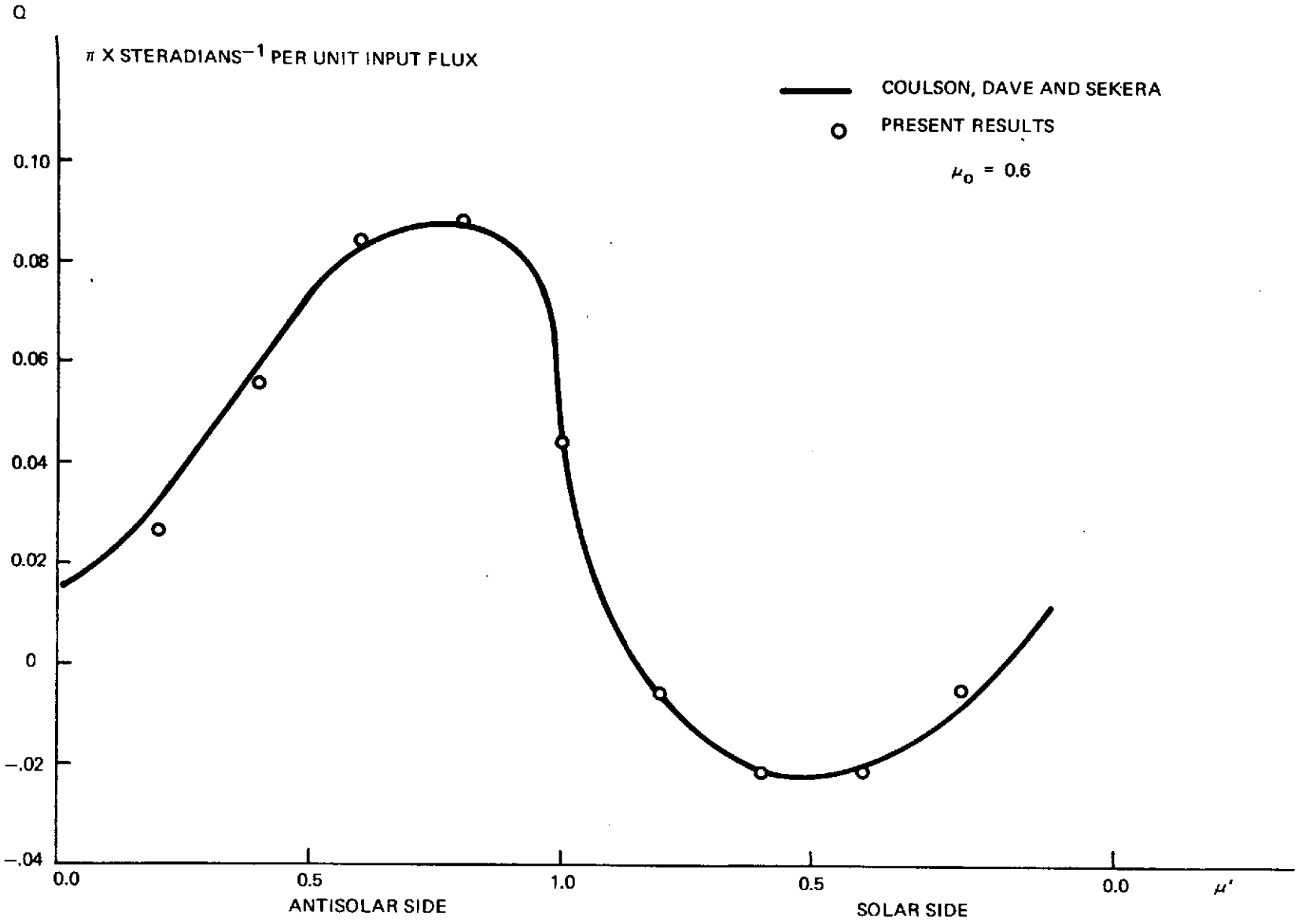

Figure 16 - Stokes parameter Q as function of zenith angle for optical thickness=1.

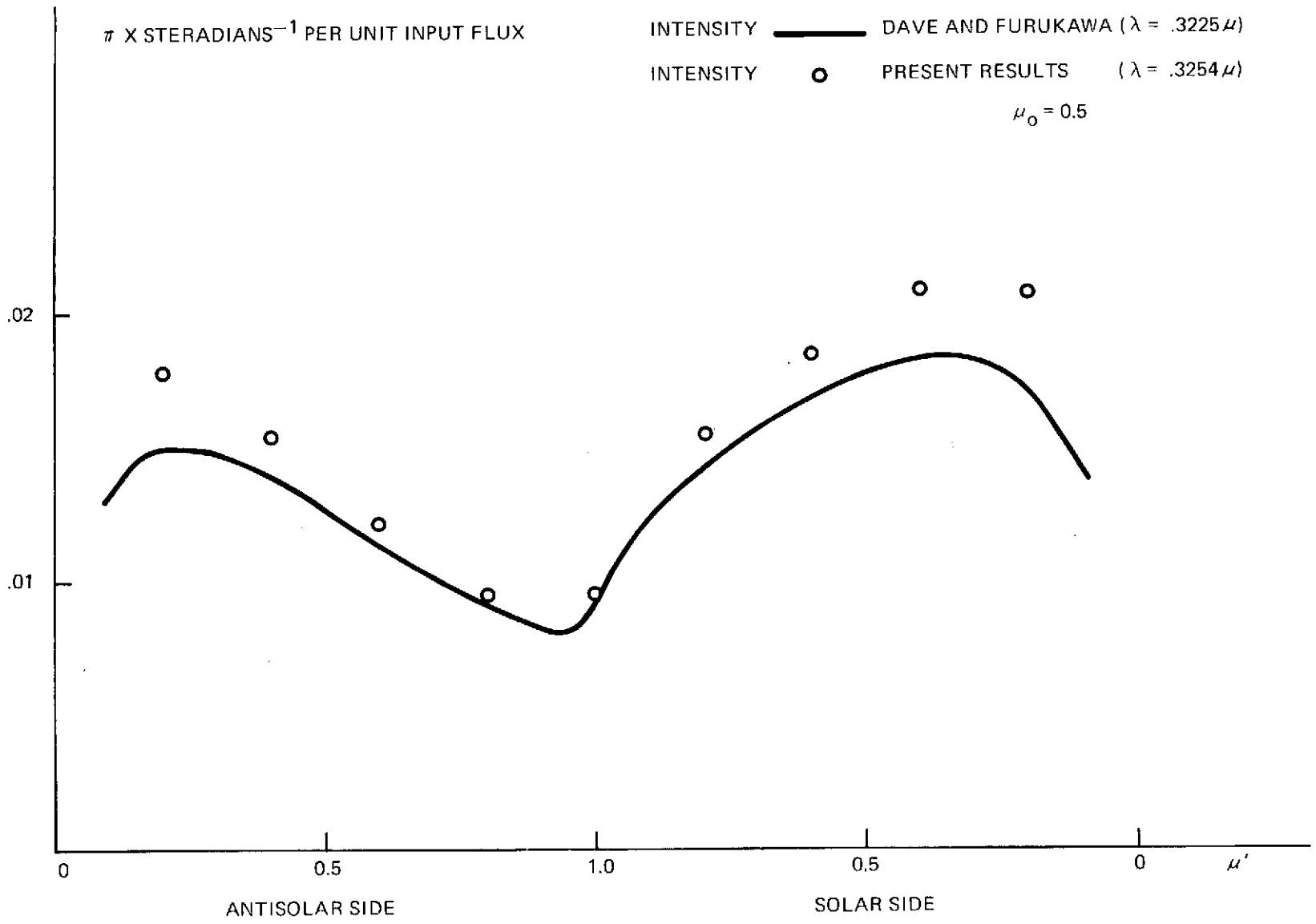

Figure 17 - Comparison of present results with Dave and Furukawa.

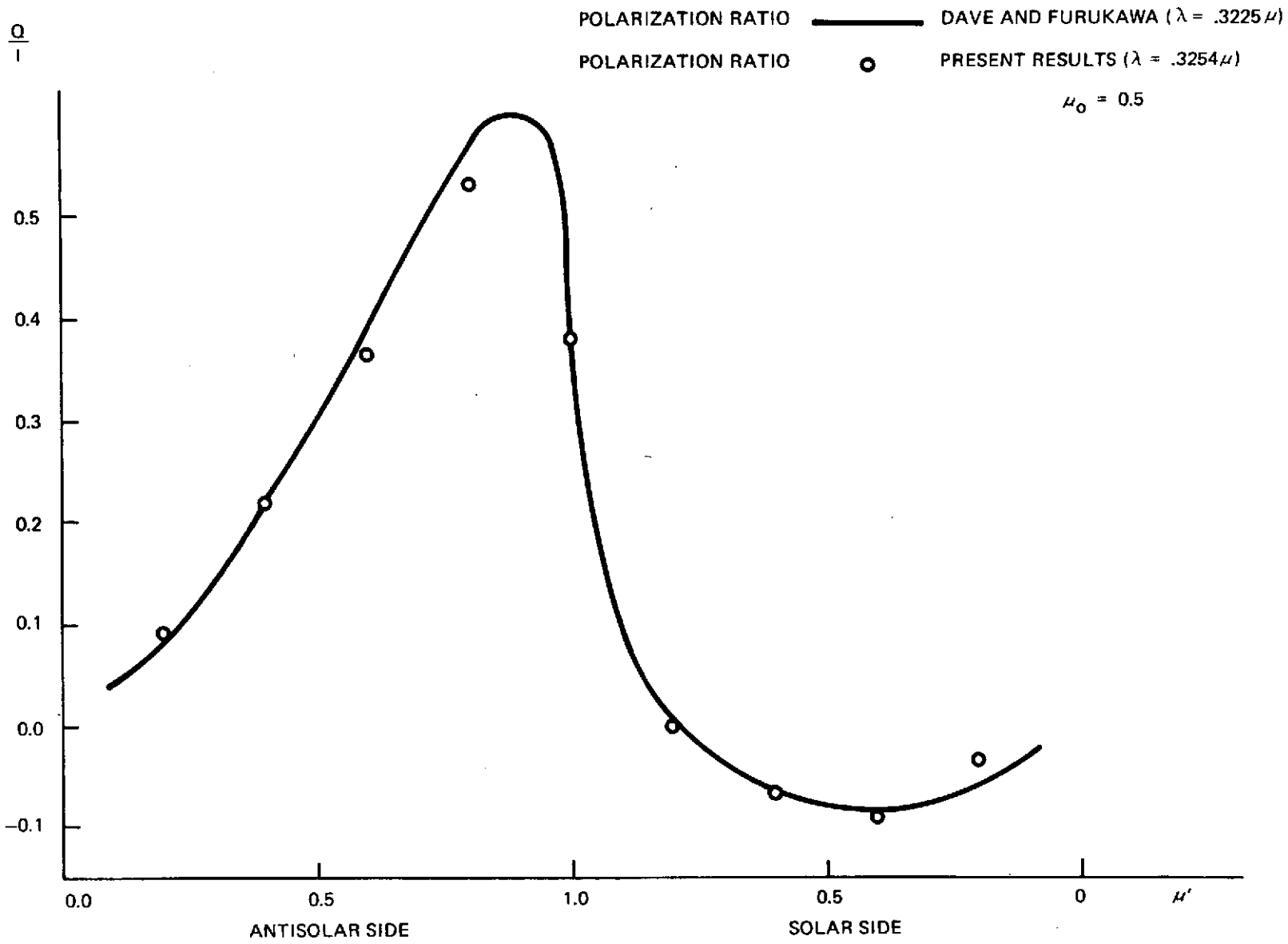

Figure 18 - Comparison of present results with Dave and Furukawa.

Discussion of Results

Using the model atmosphere presented above, we simulated radiative transfer for each wavelength in the A, C and D lines. While we were principally interested in the simulation of the Dobson spectrophotometer operating in the direct Sun mode, the versatility of the sampling routine allowed us to evaluate the intensity and polarization for zenith observations made at the ground and nadir observations made above the atmosphere at the same time. Firstly, however, we shall discuss the results for the direct Sun mode.

The parameter, N_λ, defined in equation (78), was calculated as a function of the receiver field of view using the sums of the direct and scattered intensity components. The results are shown in Figure 19. It can be seen that the effect of a finite field of view is to cause an underestimate of each of these parameters. It is relatively easy to show that the intensity due to the ith order scattering can be written as

$$I_i = K_i \tau_{sca}^i Io \exp(-\tau_{ext}).$$

where

K_i is a constant depending mostly on the field of view,

τ_{sca} is the scattering optical thickness along the slant path to the sun,

τ_{ext} is the extinction optical thickness along the same path (absorption and scattering), and

I_o is the incident intensity.

Now the values of K_i for the upper and lower wavelength will probably be nearly equal so that the relative effect of scattering can be estimated from the scattering optical thickness. Although attenuation is much more important at the lower wavelength of each line pair, it can also be seen from Table 4 that the scattering optical thickness is greater at the lower

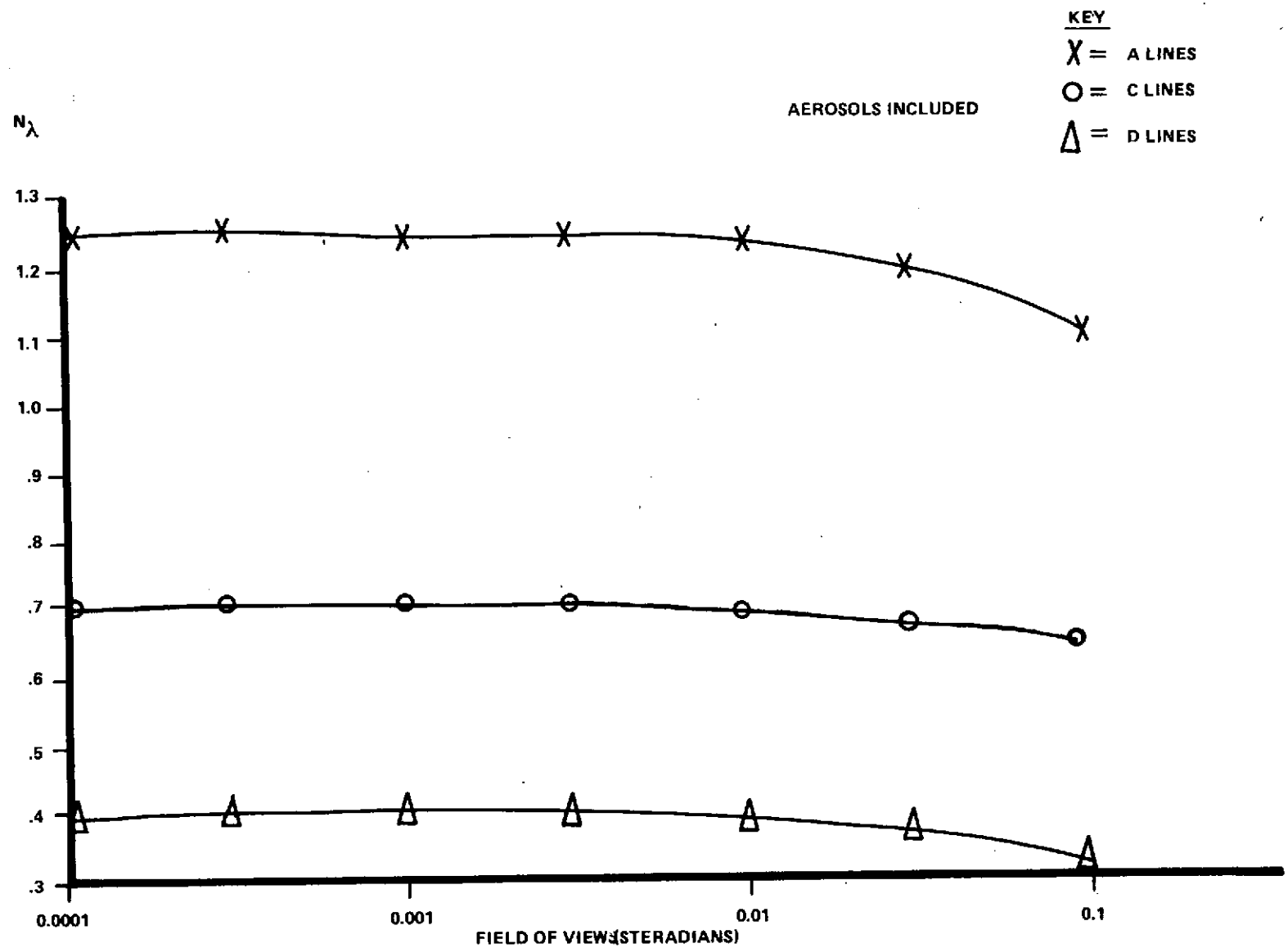

Figure 19. N_λ as function of field of view for the A, C and D lines.

wavelength also. Thus scattering is relatively more important at the lower wavelength and this accounts for the decay in N_A, N_C and N_D as the field of view is increased.

Now the true value of total ozone in the atmospheric model could readily be calculated by determining the total number of ozone molecules over one square centimeter of surface and dividing by Loschmidt's number, which is $2.69 \times 10^{+19}$ cm^{-3}. This procedure yielded

$$X = 0.36567 \quad \text{atm. cm.} \tag{83}$$

Estimates of the total ozone, X, were computed as

$$X_\lambda = (\alpha-\alpha')_\lambda^{-1} N_\lambda \mu^{-1} - \{(\beta-\beta')_\lambda m + (\delta-\delta')_\lambda \sec z\} (\alpha-\alpha')^{-1} \mu^{-1}, \tag{84}$$

where α is the mean ozone absorption cross section per atm. cm. and β and δ are defined after equation (7) on page 14. The dash refers to the upper wavelength of the wavelength pair. For zenith angles, θ, less than 60°, m and $\sec z$ may both be taken as μ, the secant of the zenith angle at the ground so that this equation may be reduced to

$$X_\lambda = A_\lambda N_\lambda \mu^{-1} - B_\lambda, \tag{85}$$

where A_λ and B_λ are constants which may be derived from the average ozone absorption cross-section and the molecular scattering cross-section. Five cases were treated:

1) A lines
2) C lines
3) D lines
4) A-D lines
5) C-D lines

It was found that when the coefficients of Table 1 which were taken from reference 1 were substituted into (85) the computed values of X_λ were significantly in error even for small fields of view. This problem was traced to a discrepancy between the mean cross sections given in Reference 1 and those of the present model. The values of the mean cross sections for ozone are computed in Table 5. When we reworked the analysis equations using our average cross sections, which are compared with those of reference 1 in Table 6, it can be seen that B_{CD} and B_{AD} are very small in both cases so that line pair coupling practically eliminates the effects of molecular scattering. We shall denote estimations made with the new coefficients as X_λ^1. The difference between X_λ and X_λ^1 indicates the sensitivity of the computed total ozone to the assumed model of ozone cross section as a function of temperature.

In Figure 20 we present the percentage errors in X_A, X_C, X_D and X_A^1, X_C^1, and X_C^1 in our simulation as a function of the field of view when no aerosol is in the atmospheric model and in Figure 21, we graph the corresponding percentage errors in X_{AD}, X_{CD}, X_{AD}^1 and X_{CD}^1. It can be seen that in this case scattering has very little effect on the results since they are insensitive to the field of view. The percentage errors in every X_λ^1 tends to zero as the field of view goes to zero indicating the validity of our analysis. Small errors occur in the X_λ values, however, emphasizing the difference between our model atmosphere cross sections and those of Reference 2.

TABLE 5. COMPARISONS OF MEAN CROSS-SECTIONS OF OZONE

	Wavelength	Cross-Section $(atm.cm.)^{-1}$	Modified Cross-Section $(atm.cm.)^{-1}$
	3055	1.882	1.883
A lines			
	3254	0.120	0.147
	3114.5	0.912	0.911
C lines			
	3324	0.047	0.041
	3176	0.391	0.382
D lines			
	3398	0.017	0.013

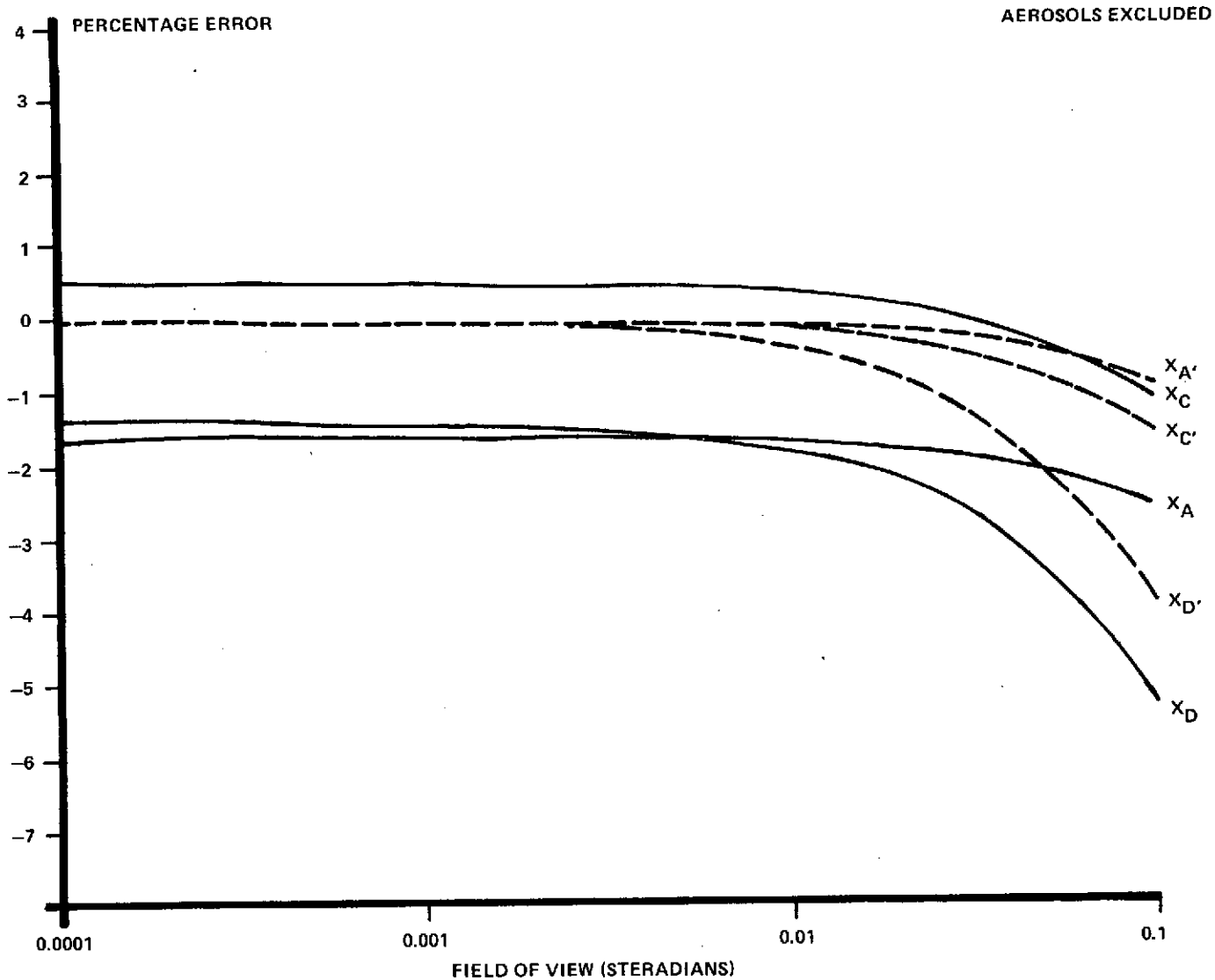

Figure 20. Percentage error in ozone estimation as a function of field of view.

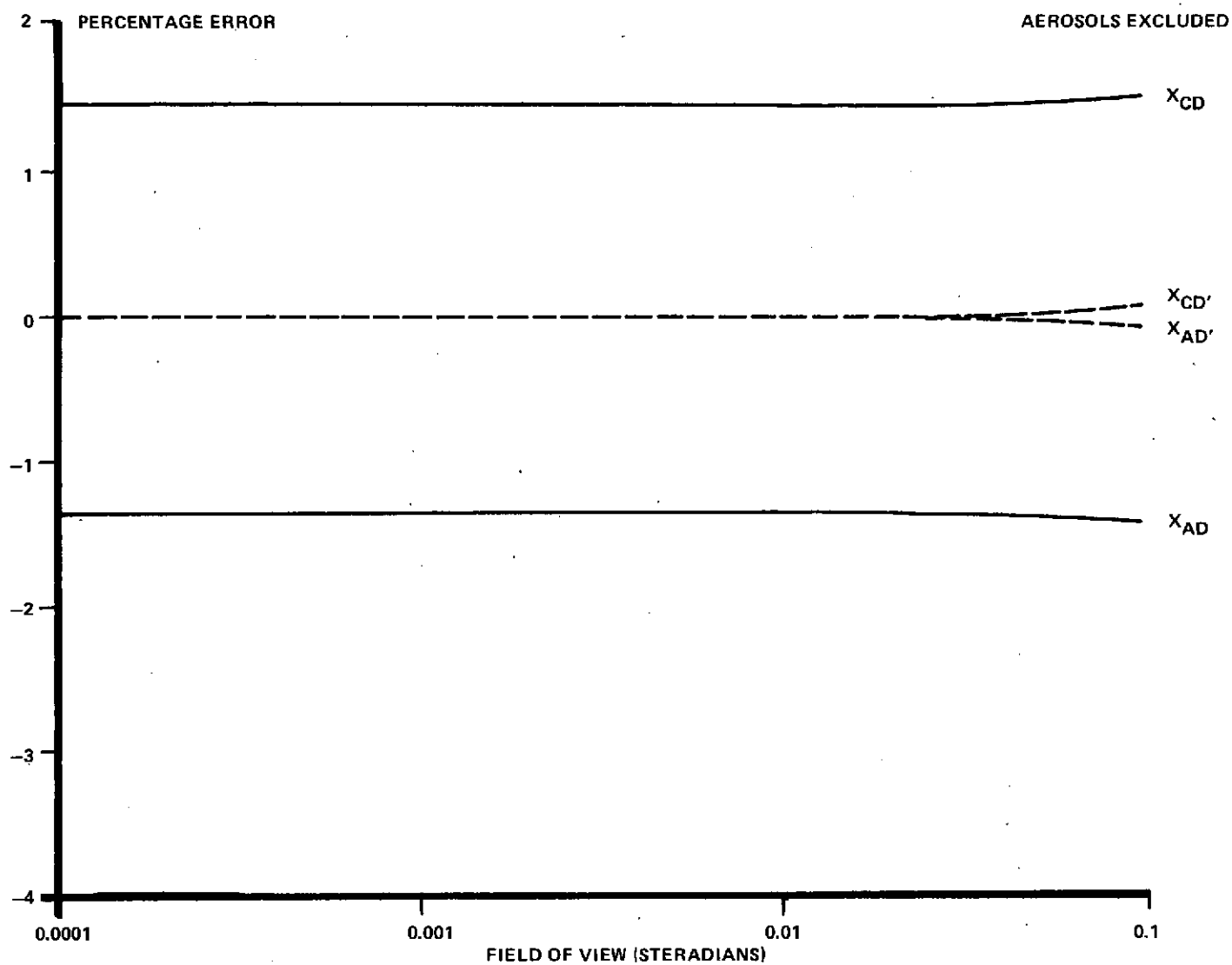

Figure 21. Percentage error in ozone estimation as a function of field of view.

TABLE 6. COMPARISON OF ANALYSIS EQUATION COEFFICIENTS

Estimation	A_λ (present)	A_λ (Ref. 1)	B_λ (present)	B_λ (Ref. 1)
A	.5761	.5675	.066	.066
C	1.1487	1.156	.124	.127
D	2.710	2.673	.278	.278
A-D	.7317	.7205	.012	.009
C-D	1.993	2.037	.006	.012

In Figures 22 and 23 we present results corresponding to those of Figures 20 and 21, respectively, but with the aerosol included in the atmospheric model. In this case the scattering effect is very noticeable and causes the total ozone estimates to be reduced by a few percent. This can be explained in terms of the forward bias introduced into the scattering by the aerosols. This considerably increases the chance that a scattered photon will travel within the field of view of the receiver either after single or multiple scattering. Multiple scattering was significant compared to single scattering in all cases.

It should be noted that X_{AD}^{1} and X_{CD}^{1} have negligible errors for small fields of view even when aerosol is present. It follows that the procedure of coupling line pairs effectively eliminates both molecular and aerosol attenuation from the analysis.

As a side calculation we evaluated total ozone from the computed zenith sky intensity ratios using the charts given in Reference 1. The results are tabulated for three cases in Table 7. It can be seen that the effect of aerosol scattering was to cause an underestimation of the correct ozone amount.

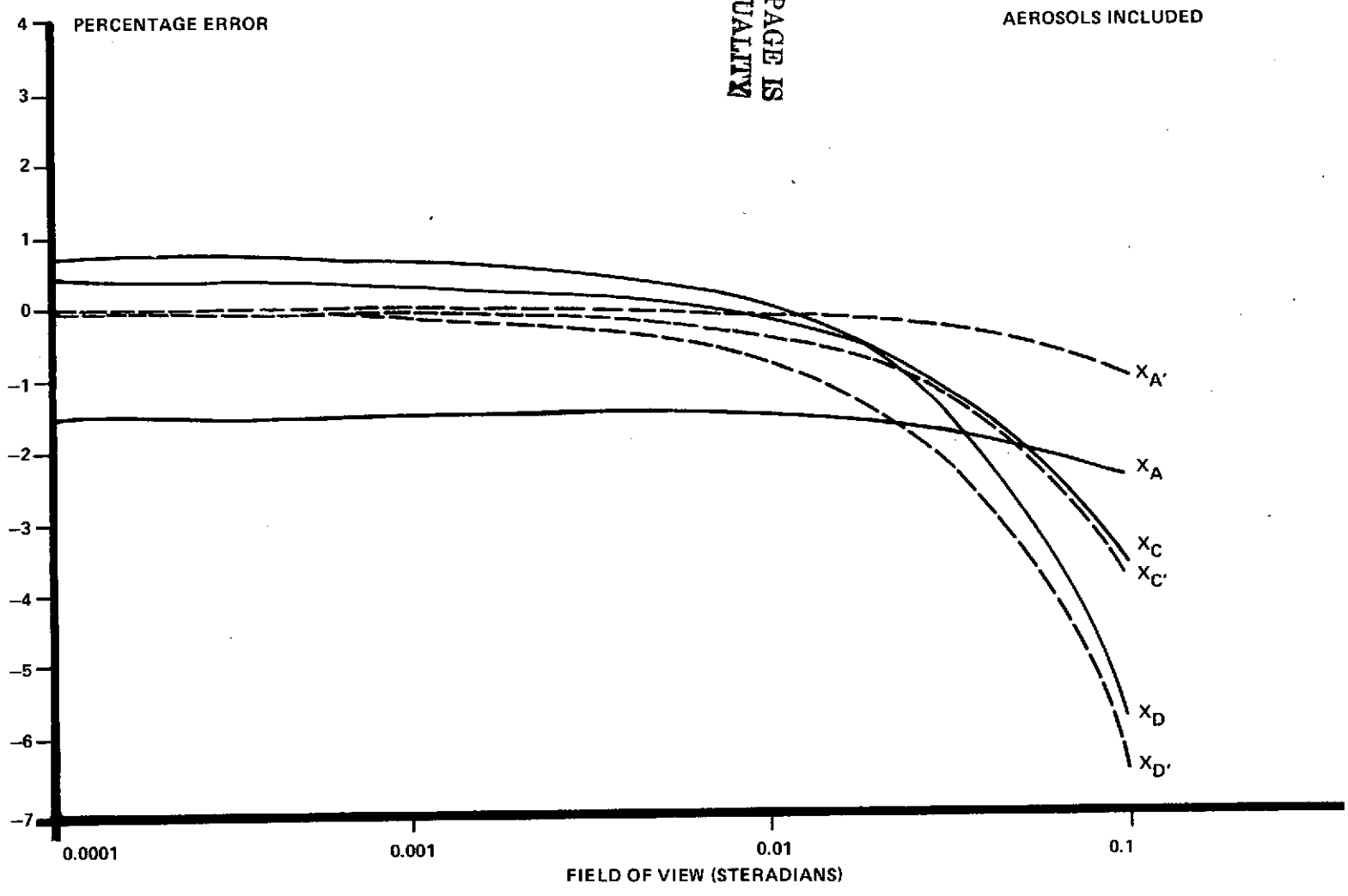

Figure 22. Percentage errors in ozone estimation as a function of telescope field of view.

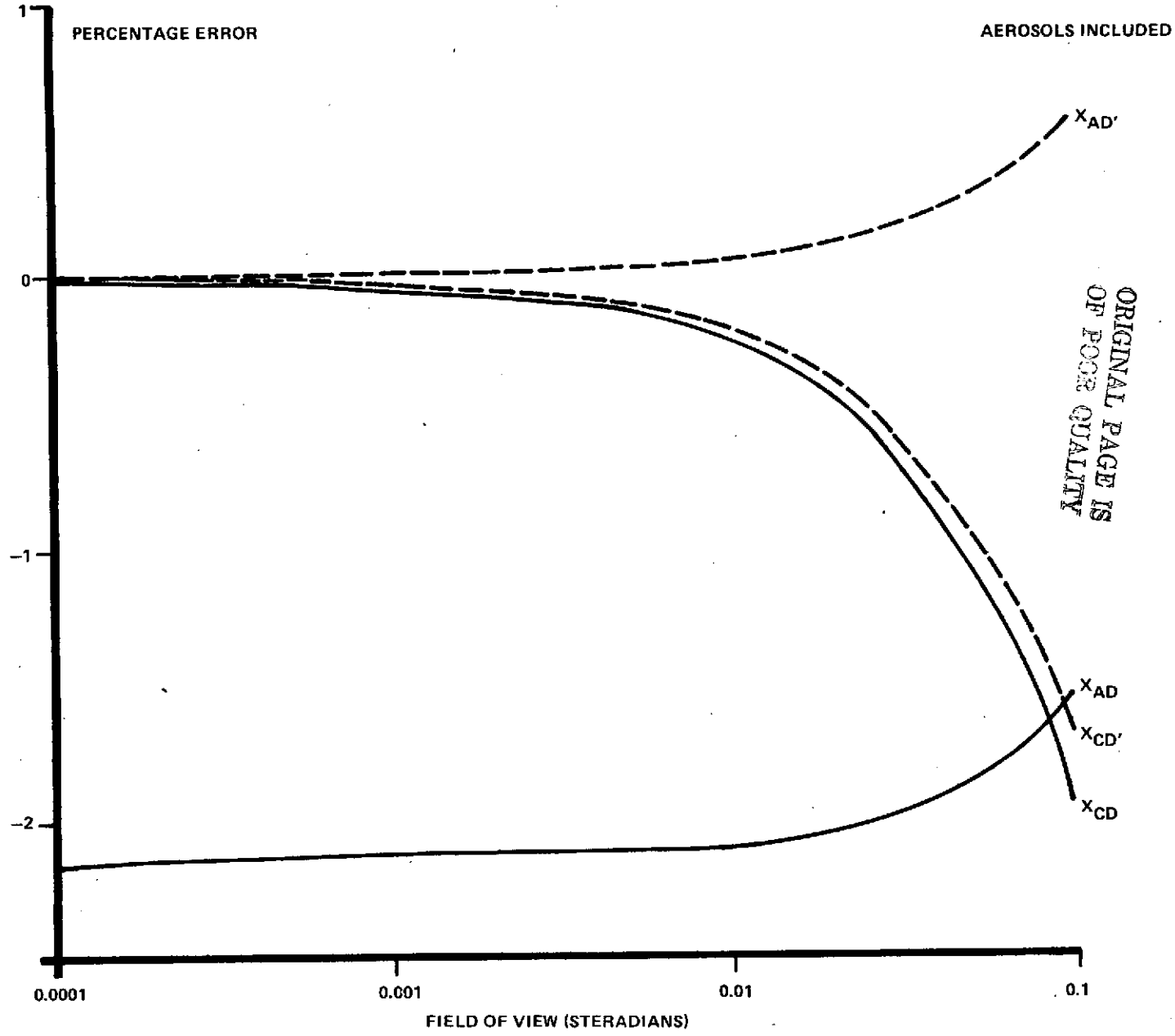

Figure 23. Percentage errors in ozone estimations as a function of telescope field of view.

TABLE 7. TOTAL OZONE ESTIMATED FROM ZENITH SKY MEASUREMENTS

Case No.	Estimated Value (atm.cms.)	True Value (atm.cms.)
1	.360	.366
2	.340	.347
3	.343	.366

These results were estimated from N_A-N_D in each case.

1. Molecular and ozone
2. Molecular and ozone (ozone profile densities reduced by 5%)
3. Molecular, ozone, and Elterman aerosol model

{cos (solar zenith angle) = 0.6}

In summary then, we have reached the following conclusions:

1) The coupling of line pairs (A,D) and (C,D) in the Dobson Spectrophotometer analysis almost eliminates the effects of both molecular and aerosol attenuation; i.e., energy scattered out of the beam. However, the effect of energy entering the beam due to scattering can be neglected only for small fields of view (less than about 5°).

2) The analysis equations depend on the temperature profile around 22 kms. since this influences the average ozone cross-section to be employed in the analysis.

3) Scattering effects are negligible when there is no aerosol. In the presence of aerosol, however, scattering effects can contribute errors in ozone estimates up to around 1% for fields of view around 10^{-2} steradians. For individual line pairs the effect of scattering is always to cause an underestimate of the total ozone, and when aerosols are present, multiple scattering is as important as single scattering.

4) The presence of aerosol can cause total ozone estimates by the zenith sky ratio to be up to 10% low.

Design and Development of Monte Carlo Simulation of Radiative Transfer Through A Spherical Shell Atmosphere

Based on the conclusions drawn from the plane-parallel model a Monte-Carlo simulation program was written to investigate radiative transfer through a layered spherical atmosphere. The details of the program are given in the Appendix and a schematic diagram of the simulation is given in Figure 24.

The surface of the earth is divided into a number of sampling annuli by selecting several ranges of sun angles of interest. In considering radiative transfer, sun angles up to 100° are allowed in order to allow for photons which may scatter back from beyond the terminator. The user will be allowed to specify the sun-angle stratifications. Obviously, the stratification density should be greatest around 90° since this is where the greatest detail is required.

It is assumed that the vertical ozone profile is uniform over the whole of the earth. Although this is not true for the real earth it will provide adequate estimations of the error due to scattering since the only requirement here is that there should be horizontal homogeneity over the region contributing to the scattering phenomenon at the localized point.

Photons are incident into zones at the top of the atmosphere corresponding to the sampling. We weight each sun angle stratification for the purpose of incident photon selection according to the solid angle presented to the sun by the associated zones.

The point of principal departure between this program and the program for the plane-parallel model is that the receivers must be localized in the sense that the sun angle must be specified. In practice, this is accomplished by averaging results for all the receivers in a given sun angle range. Care must therefore be taken to select these ranges such that significant changes in received light do not occur within any given sun-angle range.

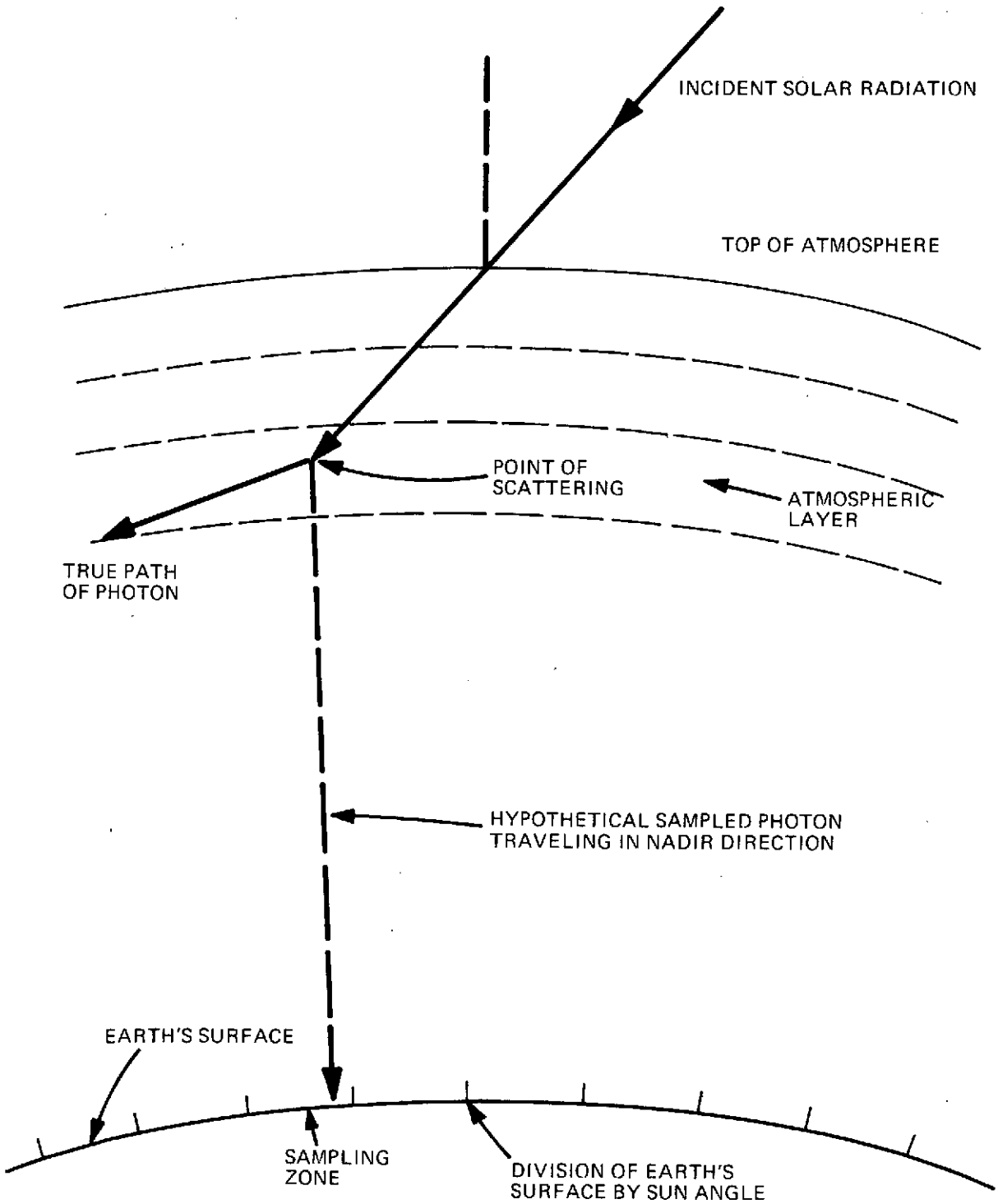

Figure 24 - Illustration of Monte Carlo method.

Essentially, the program computes the transport of photons entering the atmosphere from the sun in terms of the optical thickness measured vertically from the ground. At each encounter the particular layer of the atmosphere in which it occurs and the nature of the scatterer (molecular, ozone or aerosol) are determined in the same way as for the plane parallel model.

When the nature of the scatterer (other than ozone) has been established, we generate a series of hypothetical photons, one for each receiver pointing direction. (Most receivers are placed on the ground plane but this is not necessary.) At this point we compute the probability that a hypothetical photon would be scattered into unit solid angle of the field of view of a zenith pointing receiver beneath the scattering point and sample the Stokes vector which would be received if the event did occur weighted by the probability of occurrence for the annulus beneath the scattering point.

After sampling has occurred we return to treat the transport of the real photon to the next scattering. If the real photon reaches the ground we assume Lambertian reflection, and provided the surface albedo is not zero, it is used to compute the Stokes vector of the reflected photon. The photon tracking mechanism is terminated in one of five ways:

1) An absorption occurs.

2) The photon leaves the top of the atmosphere.

3) At the ground if the surface albedo is zero.

4) The photon is found to have suffered more than a user specified upper limit to the number of scatterings.

5) The photon reaches a location where the sun angle is greater than 100°.

The calculation at this point reverts to the next incident photon.

After a specified number of incident photons have been treated, we compute the average Stokes vector contribution for each receiver normalized to an incident flux of π photons per unit area normal to the incident beam. The number π is selected purely for convenience in matching the results of the present model with published results for the plane parallel case.

Conclusions

Our results show that in the model we have employed the total ozone estimated using the standard equations for the direct sun mode of the Dobson Spectrophotometer can be up to 15% greater than the correct value depending on the receiver field of view. The overestimate is due to two causes:

1) A discrepancy between our model of the ozone absorption cross-section and that employed by Dobson. The results demonstrate the sensitivity of the total ozone estimate to the assumed variation of total ozone cross-section with temperature, and the assumed vertical ozone and temperature profiles.

2) Single and multiple scattered radiation entering the receiver, principally radiation scattered by aerosols. The effect of scattering is to reduce the overestimation in our model.

The results for the zenith sky measurements show that in our model the total ozone is overestimated by a few percent when aerosols are not present but that the effect of single and multiple scattering by aerosols is to reduce the ozone estimate so that the overestimation is reduced.

In all of the results considered we found that when aerosols were present the effect of multiple scattering was as great if not greater than that of single scattering. Thus a detailed investigation of the influence of multiple scattering on the Umkehr experiment is necessary.

Since large solar zenith angles can be involved in Umkehr measurements it would be desirable to eliminate errors due to the earth's curvature. This can be accomplished by constructing a spherical shell atmosphere and localizing the receivers. Although the variance in the results will be larger in this model due to less frequent sampling, it is a perfectly feasible technique since the present program requires only minimal execution time. Such a model is described in the previous section.

REFERENCES

1. Dobson, G.M.B.: Ozone Spectrophotometer Operations Manual. Vol. V., Part 1, Annals of the International Geophysical Year, Pergamom Press. 1961.
2. Anon: Observers Manual, Dobson Ozone Spectrophotometer, U.S. Dept. of Commerce, Weather Bureau, Second Edition, Sept. 1962.
3. Anon: Book of Tables, Dobson No. 72, U.S. Dept. of Commerce, ESSA, Atmospheric Physics and Chemistry Laboratory, Boulder, Colorado, January 1968.
4. Anon: Ozone Spectrophotometer Adjustment and Calibration Manual, Atmospheric Physics and Chemistry Laboratory, Boulder, Colorado.
5. Anon: Instruction Manual, Electrochemical Concentration Cell Ozonesonde Model ECC-1A. ESSA-APCL, Boulder, Colorado, January 1, 1970.
6. Komhyr, W.D.; and Harris, T.B.: Development of An ECC Ozonesonde. NOAA Technical Report ERL-APCL18, Boulder, Colorado, February 1971.
7. Komhyr, W.D.: Electrochemical Cells for Gas Analysis. Proceedings of the Symposium Sur L'ozone Atmospherique, Centre National de la Recherche Scientifique, Paris, 1968.
8. Godson, W.L.: The Representation and Analysis of Vertical Distribution of Ozone. Quarterly Journal Royal Meteorological Society, Vol. 67, No. 10, October 1962, pp. 220, 232.
9. Randhawa, J.S.: Ozone Measurements with Rocket Borne Ozonesondes, Journal of Geophysical Research, Vol. 71, No. 16, August 1966, pp. 4057-59.
10. Randhawa, J.S.: Vertical Distribution of Ozone in the Winter Subpolor Region, Journal of Geophysical Research, Vol. 75, No. 9, March 1970, pp. 1693-96.
11. Randhawa, J.S.: The Vertical Distribution of Ozone Near the Equator, Journal of Geophysical Research, Vol. 76, No. 13, April 1971, pp. 8139-42.
12. Hilsenrath, Ernest; Seiden, Lester; and Goodman, Phillip: An Ozone Measurement in the Mesosphere and Stratosphere by Means of a Rocketsonde, Journal of Geophysical Research, Vol. 74, No. 28, December 1969, pp. 6873-80
13. Krueger, A.J.; Heath, D.F.; and Mateer, C.L.: High Level Ozone Distribution from Nimbus 4 and Comparison with Simultaneous Rocket Data. Paper presented at the 52nd Annual Meeting of the AGU, Washington, D.C., April 12-16, 1971.

14. Kattawar, G.W.; and Plass, G.N.: Influence of Particle Size Distribution of Reflected and Transmitted Light from Clouds. Applied Optics, 7, 869-78 (1968).
15. Collins, D.G.; and Wells, M.B.: Monte Carlo Code for Study of Light Transport in the Atmosphere. Report No. ECOM-00240-F, Vol. 1, Radiation Research Associates, Inc., 1965.
16. Elterman, L.; and Toolin, R.B.: Atmospheric Optics, Handbook of Geophysics and Space Environment, Chapter 7, Shea L. Valley, ed., AFCRL Publication (1965), pp 7-1 to 7-36.
17. Dubin, M.; Sissenwine, N.; and Teweles, S.: U.S. Standard Atmosphere Supplements. U.S. Government Printing Office, Chapter 2, (1966), pp 11-36.
18. Holland, A.C.; and Gagne, G.: The Scattering of Polarized Light by Polydisperse Systems of Irregular Particles, App. Opt., 9, 1113-21 (1970).
19. Mie, G.: Beitrage zur Optik truber Medien, speziell Kolloidaler Metallosungen. Ann. der Phys., 25, 377-445 (1908).
20. Coulson, K.L.; Dave, J.V.; and Sekera, Z,: Tables Related to Radiation Emerging from a Planetary Atmosphere with Rayleigh Scattering. University of California Press (1960).
21. Dave, J.V.; and Furukawa, P.M.: Scattered Radiation in the Ozone Absorption Bands at Selected Levels of a Terrestial Rayleigh Atmosphere. Meteorological Monograph, 7, No. 29, AMS, (1966).
22. Champion, K.S.W.: Mean Atmospheric Properties in the Range 30 to 300 km. Air Force Surveys in Geophysics No. 164, AFCRL-65-443, Air Force Cambridge Research Laboratories, Bedford, Massachusetts, (June 1965).
23. Cole, A.E.; and Kantor, A.J.: Air Force Interim Supplemental Atmospheres to 90 Kilometer. Air Force Surveys in Geophysics No. 153, AFCRL-63-936, Air Force Cambridge Research Laboratories, Bedford, Massachusetts, (December 1963).

APPENDIX
DESCRIPTION OF THE MONTE CARLO PROGRAMS AND ASSOCIATED ANALYSIS

INTRODUCTION

The Monte Carlo programs that have been written are designed to investigate radiative transfer phenomena, including polarization effects. Two separate programs have been prepared for two atmospheric geometries:

1) Plane-parallel atmospheric layers.

2) Spherical concentric layer boundaries.

Since many parts of the programs are identical, they will be discussed together. Where differences exist, the appropriate paragraphs will be prefaced by the numbers (1) or (2) assigned above. A schematic diagram of the general program schemes (applicable to both cases) is given in Figure 25 and each step in the programs will now be discussed separately.

BOUNDARY CONDITIONS AND PHOTON INITIATION

The atmosphere is characterized by a series of parallel layers whose locations are defined by the heights of their upper surfaces above the ground plane. A photon enters the atmosphere through the upper surface of the uppermost layer, with Stokes parameters $(\pi\mu_0,0,0,0)$ where μ_0 is the cosine of the zenith angle of incidence (user specified).

The ground plane is taken to be the $Z=0$ plane and the incident photon is assumed to enter in the (X,Z) plane and its Stokes parameters defined with reference to this plane. The initial direction cosines are $(\sqrt{1-\mu_0^2},0,-\mu_0)$.

The atmosphere is characterized by a series of concentric spherical shells whose locations are defined by the heights of their upper surfaces above the ground plane. A photon enters the atmosphere through the upper surface of the uppermost layer, with Stokes parameters $(\pi\mu_0,0,0,0)$. The

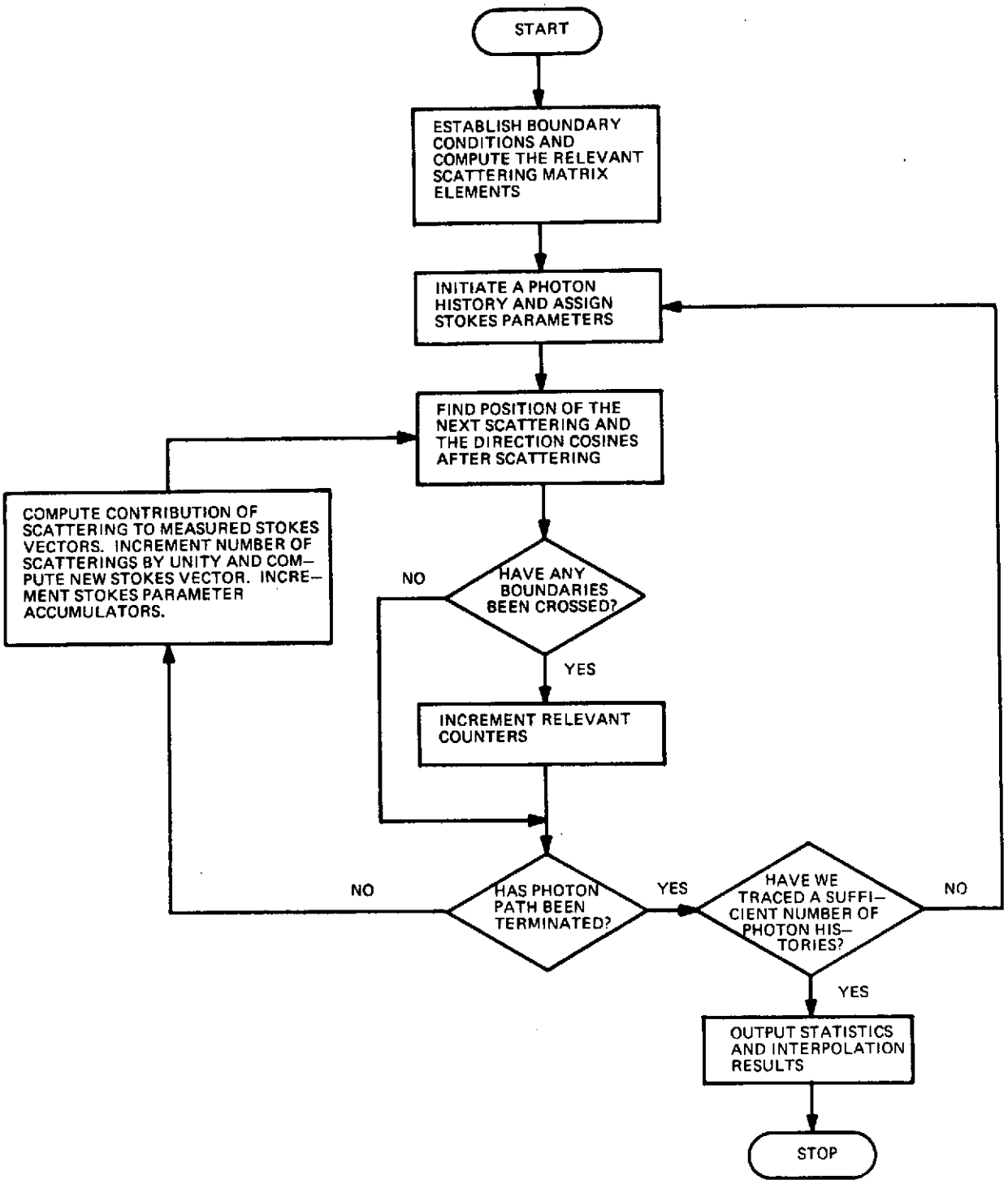

Figure 25 - Flow chart of Monte Carlo program to simulate radiation transport.

cosine of the zenith angle of incidence, μ_0, is determined at random from a quadratic distribution between 0 and 1. This provides unbiased samples for a plane parallel incident wave front.

The center of the earth is taken to be the point (0,0,0) in a (X,Y,Z) Cartesian system. The Z axis is taken to be in the direction of the sun so that the sun angle, θ, corresponding to a point (X,Y,Z) is given by

$$\cos \theta = \frac{Z}{R}, \tag{86}$$

where

$$R = (X^2+Y^2+Z^2). \tag{87}$$

COMPUTATION OF THE SCATTERING OCCURRENCE

1) Since the computations are made in terms of the optical thickness from the ground plane, this calculation is particularly easy. Suppose the photon moves from an optical thickness, λ, to a new optical thickness λ^1. Let ρ be a rectangularly distributed random number between 0 and 1 and C_Z be the Z direction cosine of the path.

Then

$$\lambda^1 = \lambda - C_Z \log_e \rho . \tag{88}$$

The altitude of the scattering occurrence may then be evaluated by table look-up techniques, matching altitude and optical thickness. The nature of the scatterer is then decided on the basis of the extinction cross sections of the components of that layer using a random selection mechanism.

2) In this case the calculation of the path length to a scattering is much more complicated than for the plane parallel atmosphere case. The reason for this is that a straight path will have varying lengths in different spherical shell layers even though the layers may be uniformly spaced.

Nevertheless, we retain the concept of computing the optical thickness τ to the next scattering by the relationship

$$\tau = -\log_e \rho \,, \tag{89}$$

where ρ is a rectangularly distributed random number between 0 and 1. Since the optical thickness per kilometer (i.e., the extinction cross section) in each layer will be known, all that will be necessary to find the next scattering is the distance covered in each layer.

A schematic diagram of the situation is given in Figure 26. A photon travels from P to Q between scatterings. P has coordinates (X_0,Y_0,Z_0) and Q has coordinates (X_1,Y_1,Z_1). The (radius, sun angle) coordinates for the points are (R_0,θ_0) and (R_1,θ_1), respectively and the direction PQ has the direction (U,V,W). The basic problem is the following:

Compute (X_1,Y_1,Z_1) given (X_0,Y_0,Z_0) and (U,V,W) as well as τ.

The first step in the solution is to consider the plane containing PQ and the origin O. Two cases must be considered:

1) The photon begins travelling away from the earth.

2) The photon begins towards the earth. In this case it is possible that the photon may graze the surface and start upwards again, but it is much more likely to reach the earth assuming it is not scattered again.

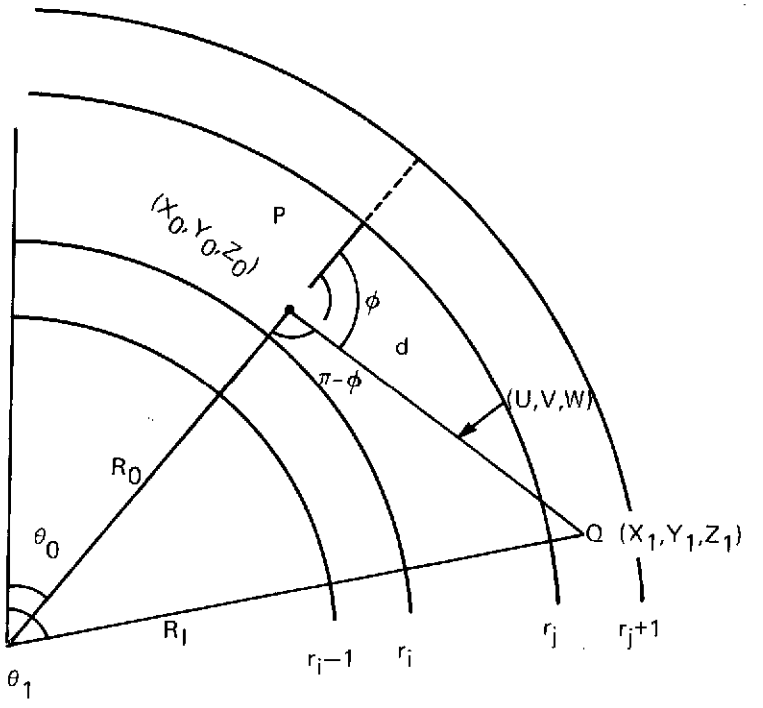

Figure 26 - Illustration of computation of scattering occurrence for the spherical geometry case.

These two cases can then be discriminated by computing the angle between (X_0,Y_0,Z_0) and (U,V,W); i.e.,

$$R_0 \cos \phi = (U X_0 + V Y_0 + W Z_0), \tag{90}$$

where

$$R_0 = (X_0^2 + Y_0^2 + Z_0^2)^{1/2}. \tag{91}$$

Cases (1) or (2) apply depending on whether this is positive or negative, respectively.

For case (1) the distance covered in reaching a radius r_j is

$$R_j = \sqrt{r_j^2 - R_0^2 \sin^2 \phi} - R_0 \cos \phi, \tag{92}$$

or using equation (90),

$$R_j = \sqrt{r_j^2 - R_0^2 \sin^2 \phi} - (U X_0 + V Y_0 + W Z_0). \tag{93}$$

Thus the distance traversed in the layer r_j to r_{j+1} is

$$R_{j,j+1} = \sqrt{r_{j+1}^2 - A} - \sqrt{r_j^2 - A}, \tag{94}$$

where

$$A = R_0^2 \sin^2 \phi. \tag{95}$$

Similarly, the distance covered in going from R_0 to r_i where $r_i < R_0$ is

$$R_i = -R_0 \cos \phi - \sqrt{r_i^2 - R_0^2 \sin^2 \phi} , \tag{96}$$

and the distance covered between r_i and r_{i+1} is

$$R_{i,i+1} = \sqrt{r_{i+1}^2 - A} - \sqrt{r_i^2 - A} . \tag{97}$$

where A is as given above.

An important parameter here is the point of closest approach to the origin (i.e., when $\phi > \pi/2$). This is given by $R_0 \sin \phi$ and the distance to the point is $-R_0 \cos \phi$. If $R_0 \sin \phi$ is greater than the earth's radius then escape is possible and the calculations, up to the radius R_0 from the minimum altitude are the mirror images of those for the descending photon.

The optical thickness of the slant path will be summed for each layer in the transit of the photon. When this exceeds τ a scattering is called. The altitude of the scattering point can then be evaluated since we know the layer in which it occurs. The nature of the scatterer is then decided on the basis of the extinction cross sections of the components of that layer using a suitably weighted random selection mechanism.

COMPUTATION OF A NEW STATE FOLLOWING A SCATTERING

The first computation at any scattering is that of the scattered direction. The distribution of scattering angles, $f(\beta)$, is completely arbitrary provided the scattering matrix elements are correctly normalized. In the computations described here we always assumed that $f(\beta)$ was proportional to the S_{11} element of the scattering matrix. This will be discussed in more detail below.

The procedure for computing the scattered direction is exactly the same as described in the earlier report. Since it is not published elsewhere, however, we shall repeat the discussion here. Let (u_I, v_I, w_I) and (u_s, v_s, w_s) be the direction cosines at the incident and scattered photon relative to a fixed Cartesian coordinate system. The direction cosine (u_I, v_I, w_I) are related to polar spherical angles θ_I and ϕ_I by the relationships:

$$\left.\begin{aligned} \cos\theta_I &= w_I , \\ \sin\theta_I &= v_I \left(1 - w_I^2\right)^{1/2} , \\ \cos\phi_I &= u_I \left(1 - w_I^2\right)^{1/2} . \end{aligned}\right\} \tag{98}$$

The scattering angle β is computed from $f(\beta)$ and an azimuthal angle ϕ generated at random assuming a rectangular relationship between 0 and 2π. The polar spherical angles θ_S and ϕ_S of the scattered beam are then estimated using the relationships:

$$\left.\begin{aligned} \cos\theta_S &= \cos\theta_I \cos\beta - \sin\theta_I \sin\beta \cos\phi , \\ \sin\phi_S &= (\psi_1 \psi_2 + \psi_3 \psi_4)\, \psi_5 , \\ \cos\phi_S &= (\psi_1 \psi_4 - \psi_2 \psi_3)\, \psi_5 , \end{aligned}\right.$$

where

$$\left.\begin{aligned} \psi_1 &= \sin\theta_I \cos\beta + \cos\theta_I \sin\beta \cos\phi , \\ \psi_2 &= \sin\phi_I , \\ \psi_3 &= \sin\beta \sin\phi , \\ \psi_4 &= \cos\phi_I , \\ \psi_5 &= (\sin\theta_S)^{-1} = \left(1 - \cos^2\theta_S\right)^{-1/2} . \end{aligned}\right\} \tag{99}$$

The new direction cosines are then computed as:

$$\left.\begin{aligned} u_S &= \cos \phi_S \sin \theta_S , \\ v_S &= \sin \phi_S \sin \theta_S , \\ w_S &= \cos \phi_S . \end{aligned}\right\} \tag{100}$$

The above relationships may readily be verified either by geometric construction or by vector analysis. In writing the coding considerable care was taken to eliminate computational redundancies since this part of the program is used more often than any other part.

The next computation at this stage is the angle, X_2, between the current scattering plane and the previous scattering plane. The absolute value of this angle can readily be obtained from the unit vector, $\underline{n}$, normal to the scattering plane and the corresponding vector $\underline{n}^1$ for the previous scattering plane using the relationship

$$\cos X_2 = \underline{n}^1 \cdot \underline{n}. \tag{101}$$

In order to establish if X_2 is positive or negative we must determine whether the reference plane is being rotated clockwise or counterclockwise when looking down the direction (u_I, v_I, w_I). This done by testing to see if $\underline{n}^1 \times \underline{n}$ has the same direction as (u_I, v_I, w_I). If this is true, then the rotation is clockwise and X_2 is positive. If not, then X_2 is negative.

The Stokes vector S_I of the incident beam is rotated so that it is referenced to the scattering plane by premultiplying by the matrix

$$\begin{pmatrix} 1 & 0 & 0 & 0 \\ 0 & \cos 2X_2 & \sin 2X_2 & 0 \\ 0 & -\sin 2X_2 & \cos 2X_2 & 0 \\ 0 & 0 & 0 & 1 \end{pmatrix} \tag{102}$$

The scattered beam Stokes vector, S_S, is then computed using the Mueller scattering matrix, normalized by the scattering angle distribution. The scattered Stokes vector in a given small solid angle $d\omega$ is given by

$$S_S = \text{constant X} \begin{pmatrix} S_{11} & S_{12} & 0 & 0 \\ S_{12} & S_{22} & 0 & 0 \\ 0 & 0 & S_{33} & S_{34} \\ 0 & 0 & -S_{34} & S_{44} \end{pmatrix} \frac{d\omega}{4\pi} S_I,$$

$$S_S = \frac{\text{constant X}}{f(\beta)} \begin{pmatrix} S_{11} & S_{12} & 0 & 0 \\ S_{12} & S_{22} & 0 & 0 \\ 0 & 0 & S_{33} & S_{34} \\ 0 & 0 & S_{34} & S_{44} \end{pmatrix} \frac{f(\beta)\ d\omega\ S_I}{4\pi}. \qquad (103)$$

Expression (A-15) applies for a perfectly arbitrary distribution $f(\beta)$. Normally $f(\beta)$ is taken to be S_{11} x a constant so that the first matrix element is always unity. This procedure has the advantage that it minimizes the variance in directions where the scattering is strongest without biasing the solution.

The scattering matrix elements for Rayleigh scattering are

$$\left.\begin{aligned} S_{11} &= S_{22} = \tfrac{3}{4}(1 + \cos^2\beta), \\ S_{12} &= \tfrac{3}{4}(\cos^2\beta - 1), \\ S_{33} &= S_{44} = \tfrac{3}{2}\cos\beta, \\ S_{34} &= 0. \end{aligned}\right\} \qquad (104)$$

SAMPLING PROCEDURE

Sampling takes place in both programs at each scattering. For each receiving region at a scattering point we compute the angle, θ , through which a scattering must take place for sampling to occur, rotate the Stokes vector to the appropriate plane, and multiply it by the normalized Mueller matrix for the scattering angle. The normalized matrix elements incorporate a weighting factor for a unit receiving area and unit solid angle. This is then referenced by rotating to the reference plane of the receiver and accumulating the individual elements for averaging later.

Normally we allow only a fixed number of potential samplings by limiting the number of scattering each photon makes before termination. This reduces inefficiencies due to computing the effects of distant scatterings.

TECHNIQUE FOR HANDLING SURFACE ALBEDO

In considering techniques for handling surface albedo it is important to retain a strong grasp of the physics of the situation at all times. The assumptions of our model of surface reflection are as follows:

1) A constant fraction of the energy incident on the reflecting surface is absorbed and the remaining fraction, A , is reemitted into the scattering medium. A is assumed to be independent of the direction of incidence.

2) The reflected radiation is completely depolarized and isotropically distributed within the half-space above the reflecting plane.

These two assumptions govern the theory of the method we employ to compute the effect of surface albedo. When a photon is incident on the reflecting surface with a Stokes vector (I, Q, U, V) a new photon is injected into the medium from the point of impact with a zenith angle θ given by

$$\cos \theta = -\rho \qquad (105)$$

where ρ is a rectangularly distributed randum number between 0 and 1. The azimuthal angle is selected randomly between 0 and 2π and the new Stokes vector is assumed to be

$$S = (2IA \cos \theta, 0, 0, 0). \tag{106}$$

referenced to any plane containing the reflected direction. The cosine term in the intensity parameter arises on account of Lambert's law, and the factor, 2 , must be included since the average value of $\cos \theta$ is $\frac{1}{2}$.

OPTIMIZATION OF THE PROGRAM EFFICIENCIES

Elimination of Redundancies. - Since a very large number of photon paths must be simulated in order to yield results with reasonably small variances, it is important to gain the maximum amount of information from each path. This is the philosophy behind the utilization of more than one sampling receiver and more than one initial Stokes vector.

Importance of Sampling. - This is a technique employed for reducing variance by limiting the computations to the areas of most interest without biasing the final estimates. This is employed as described above when the scattering angle distribution is not isotropic. The result of tracking photons, assuming isotropic scattering in this case, is that most photons soon have associated with them very small intensity parameters, and thus do not yield significant contributions when sampled. This is not a serious problem with Rayleigh scattering but can be very significant for Mie and other scatterings by particulate matter. For this reason importance sampling is employed throughout all the work described here.

C-2

Antithetic Variates. - We apply the antithetic variate variance reduction technique of Hammersley and Handscomb to generate photons with behavior characteristics that correlate negatively with each other, thus reducing the random error when the mean parameters are taken. The transports of two photons are simulated in parallel, the behavior of one being described by the random number stream ρ_i and the other by the sequence $1 - \rho_i$. Unfortunately, since many of the registering probabilities are very small this method has only limited value, however.